UNIVERSITÀ
DEGLI STUDI
DI PADOVA

Università degli Studi di Padova

Dipartimento di Scienze Chirurgiche, Oncologiche e Gastroenterologiche

CORSO DI DOTTORATO DI RICERCA IN
ONCOLOGIA CLINICA E SPERIMENTALE E IMMUNOLOGIA
XXXI CICLO

"A single-cell metabolism-based assay for circulating tumour cell enumeration and clinical validation in metastatic breast cancer patients"

Coordinatore: Ch.mo Prof. Paola Zanovello

Supervisore: Ch.mo Prof. Alfonso Colombatti

Co-Supervisore: Dr.ssa Rita Zamarchi

Dottoranda: Giulia Brisotto

To my family

Alla mia famiglia

INDEX

ABSTRACT

Breast cancer (BC) is the most common cancer among women worldwide, and it ranks as the second leading cause of female cancer-related death. To improve the clinical outcome and survival of BC patients, early diagnosis, tailored treatment and monitoring of response are critical factors. In the last decades, several studies have reported that circulating tumour cells (CTCs) could meet all these criteria. CTCs in the peripheral blood of metastatic cancer patients are associated with overall survival and treatment outcomes. A hallmark of many cancers is an altered glucose metabolism, which leads to the acidification of the tumour microenvironment. Our aim was to evaluate a method for detecting CTCs that exploits the abnormal metabolic behaviour of cancer cells in patients with metastatic breast cancer (MBC). This assay exploits a droplet microfluidic technology, which allows to compartmentalize single-cell into a droplet and detect metabolically active cells by pH measurements of the extracellular space.

Using breast cancer cell lines with different metastatic potential and normal blood cells, we established a functional cut-off, i.e.: the pH value, for discriminating CTCs from white blood cells in clinical samples. We assessed the potential of enumerating metabolically active CTCs in a cohort of MBCs and healthy donor volunteers and we compared our method to the gold standard CellSearch®. The number of detected metabolically active CTCs was significantly higher than metabolically active cells in healthy donors. Interestingly, our method was able to predict both overall and progression free survival similarly to what observed with the CellSearch, although the concordance among the two methods was not high. However, the comparison with the golden standard for CTC enumeration suggested that the two methods recognize partially overlapping populations, suggesting the combined use of both methods to better predict the patient outcome.

RIASSUNTO

Il cancro alla mammella (BC) è il tumore più comune tra le donne in tutto il mondo e si classifica come la seconda causa di decessi causati da cancro tra le donne. Per migliorare l'esito clinico e aumentare il tasso di sopravvivenza dei pazienti con BC, la diagnosi precoce, il trattamento terapeutico personalizzato e il monitoraggio della risposta alla terapia sono fattori critici. Negli ultimi decenni, diversi studi hanno evidenziato che le cellule tumorali circolanti (CTC) possono soddisfare questi criteri. La presenza di (CTC) nel sangue periferico di pazienti metastatici è associata con la sopravvivenza e la risposta al trattamento terapeutico. Una caratteristica distintiva di molti tumori è l'alterato metabolismo del glucosio, che causa l'acidificazione del microambiente tumorale. Il nostro obiettivo è stato quello di valutare un metodo per rilevare le CTC che sfrutta il metabolismo alterato delle cellule tumorali in pazienti con carcinoma mammario metastatico (MBC). Questo metodo sfrutta una tecnologia di microfluidica, che consente di compartimentalizzare una singola cellula in una goccia e rilevare le cellule ipermetaboliche mediante misure di pH dello spazio extracellulare.

Usando linee cellulari di carcinoma mammario con diverso potenziale metastatico e cellule del sangue normali, abbiamo stabilito una soglia funzionale, ovvero un valore di pH, per discriminare le CTC dalle cellule normali del sangue in campioni diagnostici. Abbiamo valutato la potenzialità di contare CTC metabolicamente attive in una coorte di MBC e donatori sani e abbiamo confrontato il nostro metodo con il CellSearch come metodo di riferimento.

Il numero di CTC metabolicamente attive è risultato essere significativamente più alto rispetto alle cellule metabolicamente attive rilevate nella coorte di donatori sani. È interessante notare che il nostro metodo è stato in grado di prevedere la sopravvivenza libera da malattia e da progressione in modo analogo a quanto osservato con il CellSearch, nonostante la concordanza tra i due metodi non fosse alta. Tuttavia, il confronto con la tecnologia di riferimento per la conta delle CTC ha suggerito che i due metodi riconoscono una popolazione di CTC parzialmente sovrapposta, suggerendo l'uso combinato dei due metodi per migliorare la predizione dell'andamento della malattia.

1. INTRODUCTION

1.1 Cancer

Cancer includes a complex and heterogeneous group of diseases that originate from cells characterized by uncontrolled proliferation and loss of homeostasis. The process of transformation of a cell from a normal to a malignant state arises from the sequential accumulation of genetic aberrations that leads to the acquisition of a spectrum of phenotypes: enhanced cellular proliferation, evasion of growth suppression and cell death signals, induction of angiogenesis, and, ultimately, activation of programmes which lead to tissue invasion and metastasis[1,2]. Further, to fulfil the bioenergetic and biosynthetic demands of continuous cell growth and survival, deregulated proliferation is accompanied by the adjustments of energy metabolism. However, the essence of neoplastic disease is not only a fact of deregulated proliferation. Indeed, tumours gives origin to complex new tissues, in which are present also stromal cells, that communicate and cooperate with one another, and immune cells with a downregulated and, in some cases, promoting tumour activity[3].

1.1.1 Cancer: future directions

Cancer is one of the leading causes of death throughout the world. As reported from the most recent World Health Organization report, cancers accounted for 8.8 million deaths and 14.1 million new cancer cases in 2012. The global cancer burden is expected to rise rapidly in the next years, estimating 21 million patients with cancer and 13 million deaths per year by 2030, because of the growth and aging of the population, as well as an increasing exposure to established factors risk such as smoking, overweight and changes in dietary behaviours and lifestyle[4]. Lung cancer is the most common cause of cancer-related death among males in countries of all incomes, and has overcome breast cancer as the leading cause of cancer death in women in developed regions; however, breast cancer is still the leading cause of cancer death among females in less developed countries[5]. Over the past few decades, advancements in the field of prevention, early diagnosis, risk stratification and therapeutic strategies have led to significant improvements in the survival of patients affected by cancer. Despite these great achievements, the metastatic spread of cancer to distant sites remains incurable, representing the main cause of cancer-related death in about 90% of cases. The investment and efforts on cancer research are unequivocally growing as reflected, for example, from the nearly quadrupled occurrence

of the term ‘cancer’ in the title of medical journal articles in the last ten years[4]. To achieve a better outcome of patients, there is the need to gain insight into tumour biology, assess more effective diagnostic strategies along with the implementation of new therapy strategies and monitoring of treatment response. Finally, the collaboration and involvement of basic and clinical research and stakeholder will be fundamental to design effective, focused and successful clinical trials to take research from the “bench-to-bedside”.

1.2 Liquid biopsy

1.2.1 Conventional cancer management

Tissue biopsies represent the standard of care in cancer diagnosis and clinical management. In cancer patients, biopsy allows to histologically define the disease and, more recently, has been exploited to assess the molecular profile of tumours; treatment strategies are defined accordingly to the evaluation of the tissue[6]. However, recent advances in next-generation sequencing technologies and bioinformatic tools have highlighted the limitations of looking at this single snap-shot provided by tissue biopsy. First, comprehensive characterization of various tumour portions taken from different regions of the primary tumours and its metastases showed that intratumour heterogeneity can occur across different regions of the same tumour (spatial heterogeneity)[7] and, as tissue biopsy only reflect a single point in time of a single site, it is likely to underestimate the complex genetic profile of a patient. The molecular heterogeneity of an individual tumour can also vary over time (temporal heterogeneity), and consequently future change in the therapeutic strategy based on historical biopsy information can result in suboptimal therapy selection[8]. Taking multiple biopsy to monitor patient’s primary tumour and metastases would seem an obvious, but not feasible, approach to face such heterogeneity. Indeed, this procedure is painful for the patient, clinically often not possible due to a high risk of procedural complications (bleeding, nerve injury or disease spreading), surgically not feasible as the tumour lesions are located at remote and not accessible sites, subject to failure in obtaining enough material of good quality for downstream molecular analysis, and expensive. The detection and management of disease relies also on serum biomarkers such as CEA and CA 15-3 for breast cancer, that, however, often lack specificity and sensitivity[9]. In clinical practice the use of these biomarkers is often coupled with imaging technologies such as computed tomography (CT), positron emission tomography (PET)/CT and magnetic resonance imaging (MRI). However, conventional imaging approaches have limited

resolution both in terms of space and time: they can reliably inform about an effective disease regression only after several weeks of treatment, subsequently delaying the chance of an earlier discontinuation of unnecessary, toxic or ineffective therapy [10,11]. In addition, conventional imaging, even if more sensitive and specific than serum biomarkers, exposes patients to ionizing radiation [12]. Consequently, there is a need for a proxy measurement that encompasses all the considered limitations, enabling a fast, minimally invasive, and cost-efficient early diagnosis, monitoring of disease status and response to treatment. In the last decades, several evidences have reported that "*liquid biopsy*" could meet all these criteria.

1.2.2 Definition of liquid biopsy

Liquid biopsy is a broad term that refers to the analysis of tumour-derived material obtained through the sampling of biological fluids of cancer patients. Although peripheral blood is the main source for liquid biopsy testing, other body fluids such as urine, saliva, pleural effusions and cerebrospinal fluid (CSF) can be used to identify circulating tumour cells (CTCs), circulating tumour DNA (ctDNA), or tumour-derived extracellular vesicles (exosome)[13]. Liquid biopsy has several advantages compared to conventional tissue biopsy. This new approach is minimally invasive as body fluids can be sampled easily, avoiding the complication of needle procedure, and repeatable over time. Moreover, as the rapid turnover of cancer cells is assumed to result in the constant release of tumour-derived material into the circulation, a liquid biopsy can in principle provide the same genetic information as a tissue biopsy, providing an alternative sample source when the conventional tumour sampling is difficult to obtain, and might offer a wider and more comprehensive view of heterogeneous cancer cells (**Figure 1**).

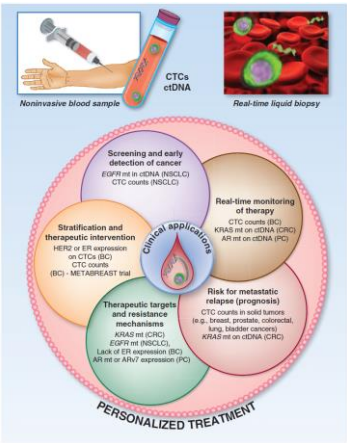

Figure 1. Clinical applications of CTC and ctDNA as liquid biopsy (adapted from [14]).

1.2.3 CTC: a background

Metastasis is the main cause of cancer related death in patients diagnosed with invasive cancer. Cancer cells that escape from the primary tumour and/or metastatic lesions, enter into the bloodstream, and contribute to forming distant metastases are referred to as CTCs [15].

Despite it has been reported that only a minority of CTCs will give metastasis, they represent an intermediate step of the metastatic process and their detailed characterization is a precious source to better understand the biology of blood-borne metastasis[16]. CTCs can be isolated from the peripheral blood of patients either as single cells or cluster of cells and their enumeration has been associated with treatment outcome and overall survival [17]. CTCs are rare events, even in patients with metastatic cancers, posing a great challenge in their isolation and detection. However, the presence of CTCs has been reported in most of epithelial cancers such as breast, lung, colorectal, pancreas, prostate and colon[13].

1.2.4 CTC and metastases

Metastasis is a complex and stochastic multi-step process that occurs through the acquisition of several phenotypes by cancer cells. Metastatic cells must invade and move from the primary tumour site; enter and survive in the circulation; arrest and extravasate at a secondary site; and finally proliferate to form secondary tumour colonies. This process can be accomplished through lymphatic and blood vessels. CTCs are believed to have a role in the hematogenous spread of cancer [16].

The metastatic cascade begins when a tumour cell acquires the hallmarks of motility and invasiveness, which confer cells the ability to separate and move away from the primary tumour mass, migrate through the surrounding tissue and then enter the bloodstream. While some CTCs might enter the blood passively, others might derive from actively invading cells that have acquired the properties of motility and invasiveness. The principal hypothesis on processes describing the intravasation of tumour cells includes the epithelial-to-mesenchymal transition (EMT) [18]. This is a concept that roots into embryogenesis as a normal evolutionary and reversible process essential for embryonic development and in wound healing [19]. Such a concept has been extended to cancer, whereby epithelial tumour cells are supposed to lose their cell polarity and cell–cell adhesion, enabling cells with a spindle-like mesenchymal phenotype and invasive and migratory properties. The activation of EMT is orchestrated by the activation of several embryonic transcription factors like

Snail, ZEB1 or Twist and paracrine signalling like TGF-beta, WNT, platelet-derived growth factors, or interleukin-6 [19]. In cancer cells undergoing EMT epithelial markers such as EpCAM and E-cadherin are downregulated and keratin expression is altered, while increased expression of mesenchymal markers like Vimentin, Fibronectin and N-cadherin is observed. In alternative to the EMT model, it has been suggested that cancer cells can detach from the primary tumours as cluster of 2 up to 50 cells. Clustered cells have a less likelihood to undergo anoikis, while they can be trapped into narrow blood vessels, thus supporting extravasation. The detection of CTCs cluster has been described for several cancers (e.g.: lung, prostate, melanoma and breast) and their enumeration associated with poor prognosis [20,21]. Moreover, they showed a survival advantage and an increased metastatic potential compared to single CTC [20].

Although it has been estimated that millions of tumour cells are released from the primary tumours, most of CTCs die in the circulation. Indeed, once in the bloodstream, CTCs have to face several natural barriers. First obstacle is shear stress forces exerted by blood. Second, CTCs must escape anoikis, an apoptosis programme that would be normally triggered by the loss of cell-matrix interaction. Third, CTCs have to evade the immune system activity. Finally, these rare cells can eventually leave the blood circulation and extravasate [18].

Extravasation starts when a single CTC or cluster of CTCs slowdown in small capillaries, attach to the endothelium, and finally undergo transendothelial migration. In most cases, the dispersed cancer cells enter a state of clinical dormancy, that is cells stop division events and, as soon as there are favourable signals and conditions, they start proliferation again. The occurrence of dormancy is mainly attributed to the EMT process, as such transition confers to cell motile and invasive properties but does not favour growth. Indeed, the reverse process of EMT, named the mesenchymal-to-epithelial transition (MET), allows a cell to acquire its initial epithelial phenotype and growth once settled in distant organs [18].

1.2.5 Detecting and characterizing CTCs

It is clear that CTCs can be considered as a fluid surrogate of cancer, as they can provide a wealth of information about the progression of disease [22]. Thus, it is not surprising that in the last decade this field of research had a boost in the development of technologies aimed at their detection and characterization. Although they were first described nearly 150 years ago [23], the first reports regarding methods for their isolation date back only to 1960s [24,25]. Research in the field had a boost when *Racila et al.* presented a highly sensitive

immunomagnetic method to enrich and detect CTCs in the late 1990s [26], demonstrating also that CTCs are present at early stage of the disease and correlates with disease progression.

A key limitation in the detection and isolation of CTCs is their low concentration in circulation compared to other normal blood cells, which poses daunting technical and analytical challenges. Indeed, it is has been estimated that 1 to 10 CTCs can be present in a background of 10^6-10^7 white blood cells (WBCs) in patients with metastatic cancer and this prevalence can decrease among different types of tumours or when considering early-stage cancers [13]. Several technologies have been proposed to isolate CTCs, usually applying the principle of "enrichment" and "detection".

1.2.5.1 Enrichment strategies

The enrichment stage (i.e.: capturing CTCs among the surrounding normal blood cells) allows to increase CTCs concentration by several log of units (positive selection) and/or depleting surrounding normal blood cells (negative selection). To date, CTC detection platforms have been developed exploiting several properties of CTCs, which include targeting of biological features (i.e.: expression of specific tumour cell surface marker) or physical characteristics (size, density, deformability or electric charges). Several CTC enrichment platforms relies on the combination of both physical and biological features (**Table 1**).

Enrichment strategy	Selection criteria	Technology	Key features	References
Immunoaffinity-positive enrichment				
	EpCAM	CellSearch®	FDA approved	[27–29]
	EpCAM	MagSweeper®	High purity; allows downstream molecular analysis	[30–32]
	EpCAM	NanoVelcro	Allows enumeration and molecular analysis at single cell level; isolated cells remain viable	[33]
	EpCAM	GILUPI CellCollector™	*In vivo* capture; can process large volume of blood;	[34,35]
	Antibody Cocktail	AdnaTest®	Captured CTCs must be lysed and tested for expression of cancer-associated tumour markers by RT-PCR	[36,37]
	Various antibodies	MACS	Positive or negative enrichment; uses magnetic nanoparticles conjugated with antibodies	[38]
Immunoaffinity-negative enrichment				
	CD45	EasySep® system	Simple and high-throughput	[39]
	Density, Antibody Cocktail	RosetteSep®	integrates density-based gradient centrifugation with immunoaffinity-based enrichment to deplete WBC	[40]
	MACS	Various antibodies		[38]
Physical-based technologies				
	Size, deformability	VyCAP	Microsieve with defined pore of 5 µm	[41]
		ISET®	Track-etched membrane with 8 µm-diameter and cylindrical pores	[42]
	Density	Ficoll-Paque®	Low cost and easy to use	[43]
		OncoQuick®	Low purity	[43]
	Electrical signatures	ApoStream®	Captures viable cells	[44]
		DEParray™	Requires pre-enrichment, allows recovery of single and viable cells through DEP cages	[45,46]
Microfluidic based platform				
	EpCAM	CTC-Chip	High recovery rate	[47]
	Size	Parsortix™	Releases viable cells	[48]
	Size deformability	Vortex	Captures viable CTC, does not require blood lysis	[49,50]

Table 1. Table summarizing few of the existing platforms and strategies for CTC enrichment.

1.2.5.1.1 Protein expression-based technologies

The most successful and widely used approach for isolating CTCs is based on the affinity of a specific biomarkers expressed on the cell surface of CTCs to a corresponding antibody.

This CTC enrichment strategy is usually carried out by using magnetic beads coated with antibodies specific for a tumour antigen and the antigen-antibody complex is subsequently isolated by a magnetic field. Epithelial markers are usually expressed on cancer cells of epithelial origin, while are absent on the mesenchymal leukocytes and therefore they have been widely applied to discriminate cancer cells from normal blood cells.

The cell surface marker that has been most frequently used for positive CTCs selection is EpCAM. Among the EpCAM-based immunomagnetic enrichment methods, CellSearch® (Menarini, Bologna) is the only FDA-approved platform for *in vitro* diagnostic use in patients with metastatic breast, colorectal or prostate cancer and, notably, is still considered the gold standard among the CTC detection methods [51]. In this system CTCs are defined as nucleated cells positive for cytokeratins (CK) staining and negative for the common leukocyte antigen CD45. A threshold of ≥5 CTCs in a 7.5ml of blood for metastatic breast and prostate cancers, and of ≥3 CTC for colorectal cancer has been proven to be associated with decreased progression-free and overall survival [52].

Other examples of innovative EpCAM-based technologies are the MagSweeper® (Illumina, San Diego, CA), which isolates CTCs by using antibody-coated magnetic beads and a magnetic rod, and the "NanoVelcro" CTC chip, a nanostructured substrate with silicon nanowires which allows high recovery and release of captured CTCs [30–32].

Another issue limiting the sensitivity of CTC detection is the sample blood volume that has to be processed *ex vivo* [53]. An interesting commercially available *in vivo* capture device has been introduced by GILUPI Gmbh (CellCollector®). This device consists of a guidewire covalently functionalized with anti-EpCAM antibodies, which is positioned directly in the arm vein of cancer patients and trapped CTCs are detected and evaluated by immunocytochemistry. Recently, *Gorges T.M. et al* have also demonstrated the feasibility of downstream molecular analysis of these captured CTCs [34].

However, cancer cells might undergo EMT with a subsequent downregulation of epithelial markers (e.g.: EpCAM) thus, targeting such surface marker, might result in an underestimation of the total CTCs and subsequent false-negative findings. In addition, increasing evidence highlighted also the importance of stem cell marker in CTCs. A response to such a need has been the introduction of expanded antigen repertoire to capture CTCs by including mesenchymal markers (e.g.: N-Cadherin and Vimentin), stem cell markers (e.g.: CD133 or CD44) and cancer- or organ-specific markers (e.g.: HER2, PSA or EGFR). The AdnaTest (Adnagen AG) is an example of commercially available assay, which enables a broader capturing approach by using cocktail of antibodies (e.g.: EpCAM,

HER2, MUC1) bound to magnetic beads and specific for cancer type. A limitation of this test is that captured CTCs must be lysed to be tested for expression of various cancer-associated tumour markers using RT-PCR, limiting the possibility to perform other downstream analysis such as single-cell NGS.

Positive enrichment strategies can attain high recovery and purity rates, but their performance depends on both the degree of expression and specificity of target antigen, as well as on the binding quality of the associated antibody and the labelling process.

Negative enrichment technologies circumvent some of the pitfalls of positive selection. This strategy uses an indirect method to detect CTCs by targeting and depleting unwanted background cells, such as leukocytes, red blood cells and platelets. This approach is often preferred because, without labelling CTCs, it does not introduce biases to the sample according to the used selection marker [54]. A downside of the negative selection is the lower purities achieved compared to positive enrichment. However, depletion methods offers the possibility to obtain unlabelled CTCs that can be further employed in further analysis [22].

The most widely used marker for WBC depletion is CD45. Examples of negative selection are the EasySep® system (STEMCELL Technologies, Vancouver, Canada), which depletes unwanted cells using magnetic nanoparticles and tetrameric antibody complexes against CD45 and the RosetteSep® (STEMCELL Technologies), a mixture of antibodies that crosslink CD45-expressing leukocytes to red blood cells in whole blood, forming cells rosette complexes.

In addition, many systems involved in the positive enrichment are able to work for the negative counterpart by applying different antibodies, for example replacing anti-EpCAM with anti-CD45 (e.g.: MACS®, MagSweeper®).

1.2.5.1.2 Physical-based technologies

Another approach for CTC enrichment is to target them by physical properties (size, density, deformability and electric charge) that are supposed to be unrepresented in the normal cell populations. These strategies are commonly referred to as “label-free” method and have recently gained great attention from the field. The main advantage is that captured CTCs are not tagged with an antibody, which can be useful in downstream processing.

Size-based CTC enrichment technologies have been developed on the observation that CTCs have generally larger morphology respect to WBCs[55]. Downsides of this approach are a low sensitivity and specificity as the existence of smaller CTCs has been demonstrated

[48,56]. Filtration enables enrichment of CTCs exploiting cell size. Examples of such approach are VyCAP or ISET® (RARECELLS US) [41,42].

Density gradient centrifugation is a conventional method for separating blood component based on a cell specific coefficient of sedimentation. Ficoll-Paque® (GE Healthcare Life Sciences) and OncoQuick® (Grenier BioOne) are the most widely used system, which allows to separate CTCs from erythrocytes and granulocyte. These methods are reliable and inexpensive but suffer the disadvantages of non-specific loss of target cells, due to the presence of CTC with density comparable to WBC, and insufficient purity for most of the downstream analysis [43].

Dielectrophoresis (DEP) relies on the distinct electrical fingerprints of different cells, which depend on the cell morphology and membrane surface area. A non-uniform electric field applied by an array of electrodes causes a differential movement of the cells depending on their dielectric properties. ApoStream® (ApoCell) is a commercial system for CTC enrichment, which employs this strategy to effectively isolate CTC from clinical samples [44,57]. While this strategy recognizes cells based on their dielectric properties, DEP can also be applied as a technique to finely manipulate and move single-cells detected with other methods. In this context, the DEPArray system (Silicon Biosystems) deposits single cells in DEP cages generated with electric field and is able to gentle recover in a tube single and viable cells for subsequent characterization [58].

1.2.5.1.3 Microfluidic Methods for CTC Capture

Microfluidics offer the possibility to precisely control small volumes of fluids (down to a picoliter), by using device with channel dimensions of ten to hundreds micrometers, and to simultaneously handle multiple samples in multiple bioreactors (Whitesides, 2006). Soft-lithography and polydymethylsiloxane (PDMS) have become the most widely represented methods for fabricating microfluidic devices for biological application as PDMS is flexible, allowing easy and rapid fabrication of devices with various architecture; transparent, providing excellent live cell imaging conditions and permeable to oxygen, essential for cell survival [59,60]. In summary, microfluidics present several essential advantages including reduced sample volume and reagent consumption, fast processing and low cost, highlighting its clear potential to be applied in several biological areas, such as cancer research.

Over the last two decades, microfluidic technologies for isolating CTCs have attracted great interest because of their ability to isolate CTCs exploiting various physical and biological features[61] and combine isolation and detection methods in a single device.

In 2007, *Nagrath et a*l. have described the first microfluidic platform for CTC detection, that consists of EpCAM-functionalized microposts for capturing CTCs from whole blood with high sensitivity and purity [47]. The CTC-Chip has undergone several improvements like the development of geometrically enhanced microstructures aimed at increasing the degree of purity of CTC while maintaining a high recovery efficiency [62].

Other promising platforms are the Parsortix™ system (Angle), consisting of a disposable cassette with a stair-like architecture that retains into the system only larger CTCs, or the Vortex HT chip, a device with rectangular reservoir in which laminar fluid microvortices are generated at high flow rates to quickly and passively enrich CTCs at high purity from a large volume of blood and concentrate these cells in a small volume [48].

1.2.5.2 CTC detection method

Detection of CTCs (i.e.: verification of identity of captured cells) is commonly performed either morphologically by immunostaining and microscopy or at the molecular level by PCR-based method[63].

1.2.5.2.1 Direct imaging

A widely used method to verify the nature of captured cells is achieved through staining of cells with tumour-specific antibodies followed by high resolution imaging. While CTC staining allows a valuable enumeration of CTCs, this approach is limited by the number of antibodies that can be employed for visualising cells of interest. Further, despite enrichment strategies lower the number of cells to be analysed, imaging is time-consuming and needs a laborious operator-dependent scoring. To overcome these issues, several technologies have integrated automated high-resolution fluorescence imaging into their workflow. An example is the open-source software ACCEPT coupled with CellSearch® [64,65]. The HD-SCA assay (EpicScience, San Diego), in combination with a custom-made software, allows to screen monolayer of millions of nucleated cells plated on customized glass slides. Advantages of this platform are the unbiased selection of CTCs, as no pre-enrichment step is required, and the possibility to perform molecular characterization at the single-cell levels[66]. However, a drawback is that cells need to undergo a step of cell fixation and thus no viable CTCs can be recovered for further analyses [22].

1.2.5.2.2 Functional assay

Functional assay takes advantage of viable cells properties for enrichment and detection of CTCs [54]. In principle, detecting viable cells in the peripheral blood of patients would be highly desirable, as only functional cells can contribute to the process of metastasis. The Epithelial ImmunoSPOT Assay (EPISPOT) is an enzymatic assay which capture CTCs exploiting the secretion, shedding or active release of tumour-associated proteins from different cancer cells put in culture for 24-48 hours; for example, CK-19 and MUC1 can be exploited in the case of breast cancer, or PSA for prostate cancer sample [67,68]. Vita-Assay™ (Vitatex, New York) is another functional assay based on the ability of tumour cells to invade a collagen matrix *in vitro,* and it has been tested in breast, ovary, prostate, pancreas, colorectum, and lung cancer [69].

An interesting approach is the study of ex vivo isolated CTCs is their transplantation into immunodeficient mice to obtain CTCs derived xenograft (CDX) [70–72]. This has been achieved with CTCs obtained from patients with luminal breast cancer [73]. Similarly, *Hodgkinson et al* obtained a CDX model by using CTCs from patients both from chemosensitve and chemorefractory small cell lung cancer which mirrored the response to therapy and had a comparable genomic profile of the donor patients [71]. Establishing permanent cell lines from CTCs has also been explored, even if with scarce result. To date, only one cell line has been obtained and characterized using CTCs from one patient with colon cancer [74].

1.2.5.2.3 Molecular characterization

The recent prevailing aim in CTC characterization is the analysis of their genomic content, as they can provide clinically valuable information about the mutational status of the tumour. Before performing any other downstream analysis such as mutational analysis of therapeutic target genes, copy number variation analysis or exploration of new druggable mutation, DNA-based technology might require whole genome amplification (WGA) to increase the amount of copy numbers to be analysed. However, this process might introduce bias derived from DNA amplification leading to false positive results and thus comparative studies between CTCs and normal cells are highly suggested.. For instance, coupling CellSearch and DEParray, single CTCs and WBC were obtained from metastatic breast cancer patients and after amplification with WGA, the mutational status of PI3KCA were assessed demonstrating the feasibility of the approach to detect hotspot mutations and the heterogeneity among CTCs [75]. Further, mutations in KRAS, which can impede the EGFR-

targeted therapy efficacy in colorectal cancers, revealed the heterogenous presence of KRAS mutations[76].

RNA-based technologies are very promising. Gene expression analysis are widely performed by using fluorescent in situ hybridization (FISH)[77], real-time PCR, microarray mRNA sequencing. Recently, also transcriptome analysis has been successfully applied on isolated CTCs. Asingle-cell RNA-sequencing profile of isolated CTCs from prostate cancer patients have displayed the activation of a non-canonical Wnt signalling pathway in patient who progressed under treatment with an AR inhibitor, respect to untreated patients[78]. Recently, *Kalinich et al* demonstrated the feasibility of applying RNA-based digital PCR in the assessment of a panel of genes in CTCs derived from hepatocellular carcinoma (HCC) [79].

Overall, the field of detection and characterization of CTCs have increased enormously and the approaches to characterize them are very numerous. However, at present, there is no perfect technique as each of them presents limitations. Therefore, several groups of research have started to explore the combination of methods based on different properties, aimed at finding the perfect combination to obtain a pure and functional CTC population [22].

1.2.6 Requirements for developing a CTCs platform for clinical application

The characterization of CTCs holds the appeal and the potential to improve cancer diagnosis and prognosis as well as to enable a more sensitive real-time monitoring of the disease for guiding treatment decision of individual patients. Therefore, it is not surprising that a plethora of promising and innovative methods have been developed in recent years to capture, enumerate and characterize them. As described in the previous section, several strategies for CTC detection have been proposed. This long list highlights the lack of a consensus about the most appropriate method for detecting these rare cells as well as a clear definition of their phenotype or the identification of a perfect marker for their selection. These requirements have led to the definition of a standard set of performance criteria, such as capture efficiency, purity enrichment and throughput, aimed at evaluating and comparing all the different technologies (**Table 2**). Of note, all these measurements to estimate CTC platform sensitivity are assessed by spiking cells from cancer cell lines into healthy donor blood sample (i.e.: adding a known number of tumour cells derived from commercially available cell lines into blood samples). However, cancer cell lines do not outline the actual physical and biological heterogeneity of CTCs like size, protein expression or stiffness, but

tend to be more homogeneous and more physically different from leukocytes than patient CTCs. Therefore, on one side, spiking assay might overestimate the real device performance, but, on the other side, patient samples cannot be directly used for a preclinical validation of the device as the real number of CTCs in a clinical sample is always unknown [54]. Since there is a lack of a reference method to enumerate CTC, direct comparison between techniques on clinical samples could be more valuable and CellSearch is often used as the reference technique [80,81]. Moreover, the increasing interest beyond the simple enumeration of CTCs has resulted in the development of technologies that enables obtaining samples suitable for molecular downstream analysis of CTCs. Genomic and transcriptomic downstream analyses might require cell viability, although not always, but they do need high purity because contaminating DNA or RNA from WBCs can alter results. Thus, two additional performance metrics have been introduced: i) cell viability, the percentage of capture tumour cells that are still alive after enrichment, and ii) release efficiency, the percentage of captured target cells that can be recovered from the device.

Despite the great potential of applying CTCs as biomarker in cancer, such approach is still not widely adopted in the routine clinical care as only a few of these technologies report the stringent clinical validation required before their introduction into the clinical management of cancer. Before any technology could be used in medical decision making in a specific context of use, demonstration of analytic validity, clinical validity, and, most importantly, clinical utility is required. Analytical validation begins with the discovery of the biomarker to be developed and the implementation of a robust assay that provides reproducible results across several testing laboratories and systems. This step includes the definition of easy-to-use workflows spanning from the pre-analytical phases (e.g.: specimen collection and transport) to the data analysis and interpretation of results [51,82]. After demonstration of analytic validity, the clinical validity can be explored. Firstly, the context of use has to be defined (i.e., diagnostic, prognostic, predictive, or surrogate of efficacy of response). Then, the value of the test to predict specific clinical outcome has to be assessed. Finally, the clinical utility has to be performed, that is provide the demonstration of the capacity of the test to impact on the outcome of the patients[51].

PERFORMANCE METRICS	DESCRIPTION	DEFINITION
CAPTURE EFFICIENCY (OR RECOVERY RATE)	The ability of the device to capture cancer cell lines from spike blood samples	$\frac{(Target\ cells)_{\ CAPTURED}}{(Target\ cells)_{\ SPIKED}}$
PURITY	Capacity of the system to specifically capture tumour cells within a background of contaminating cells (usually WBC) before and after running the sample into the device	$\frac{(Target\ cells)_{\ CAPTURED}}{(Target\ cells + WBCs)_{\ CAPTURED}}$
ENRICHMENT	Factor of enhancement of the target cells respect to the background at the output of a system respect to the input	$\frac{\frac{(Target\ cells)_{\ CAPTURED}}{(WBC)_{\ CAPTURED}}}{\frac{(Target\ cells)_{\ ACTUAL}}{(WBC)_{\ IN}}}$ **or** $Capture\ efficiency \times \frac{(WBC)_{\ CAPTURED}}{(WBC)_{\ IN}}$
THROUGHPUT	Described how quickly a device can process a sample	$\frac{n°\ of\ cells\ processed/}{unit\ time}$ **or** $\frac{volume\ of\ sample\ processed}{unit\ time}$

Table 2. Metrics for measuring the performance of CTC enrichment platforms.

1.2.6.1 Clinical validity of CTC

The value of CTCs detected by CellSearch® as a prognostic factor of clinical outcome have been extensively reported in metastatic and localized carcinomas in a series of prospective clinical trials. In 2004, the pioneering work from *Cristofanilli et al*. demonstrated that CTC count detected by CellSearch® was an independent prognostic factor for progression-free survival (PFS) and overall survival (OS) in metastatic breast cancer [27]. The established cut-off of ≥5 CTC/7.5 ml of blood to discriminate between patients with good or poor prognosis in metastatic breast cancer has been further validated in several studies [28,29,83]. Beyond breast cancer, a number of CTCs higher than a specific cut-off levels and its correlation with poor prognosis have been validated also for metastatic prostate (≥5 CTC/7.5 ml) and colorectal cancer (≥3 CTC/7.5 ml) [52,84,85]. Interestingly, at the follow-up after the beginning of a new therapy, several studies have shown that a decrease of level of CTC count enabled prediction of treatment efficacy [28,86]. The prognostic utility of CTCs has been explored also in NSCLC (cut-off level of 5 CTC/7.5 ml of blood) and SCLC (≥50 CTC/7.5), in which the number of CTC is the ever most abundant described until now [21,87]. Also, for metastatic lung cancer, CTCs showed their potential as a pharmacodynamic biomarker, beyond its use as prognostic marker. Moreover, CTCs have been detected before and after surgery of several non-metastatic cancers such as breast [88] and colorectal [89,90]. In locally advanced breast patients, monitored for CTCs before and after neoadjuvant

treatment, *Riethhdorf et al*. showed that detection of CTCs before therapy is an independent prognostic factor of impaired clinical outcome [91].

1.2.6.2 Clinical utility of CTCs

Although the presence of CTCs has an undoubted prognostic value, the clinical utility of CTCs remains controversial. This means that there is the need to design prospective, randomized multicentre clinical trials to demonstrate that CTCs evaluation can impacts on patient outcomes.

CTCs might be a marker of treatment response. In this regard, the SWOG S0500 (NCT00382018) clinical trial was designed to determine whether MBC patient switching to another treatment, in case of high CTC number after the first cycle of therapy, could benefit patients in terms of OS. The results showed that this early change of therapy did not improve either PFS or OS [92]. The authors claimed that the lack of improvement is probably due to a general chemoresistance of the studied population and that there would be the need of more effective therapeutic agents at the time of progression, rather than persisting with further lines of standard chemotherapy.

CTCs have the potential to provide also insight into the presence of marker for treatment sensitivity. For example, the presence of the splice variants androgen-receptor splice variant 7 (ARV7) can be used as a biomarker for resistance to enzalutamide and abiraterone therapy in prostate cancer patients. Recently, the presence of ARV7 in CTCs have been detected in patients with metastatic prostate cancer. The positivity for ARV7 predicted resistance to therapy, along with a shorter PFS and OS compared to ARV7 negative patients[93].

1.3 Cancer metabolism

Metabolism is a general term used to describe a group of biochemical reactions that happen within a living organism to sustain life. Metabolism can be divided in two types of reactions: *catabolism*, which refers to the breakdown of complex molecules into smaller molecules to extract energy and produce ATP, and *anabolism*, which describes the consumption of energy to catalyse the production of complex macromolecules needed for cell survival and proliferation [94]. To satisfy the demands of uncontrolled proliferation, cancer cells require large amount of nutrient uptake and metabolism to meet both catabolic (ATP-producing) and anabolic (biomass-synthetizing) demands. Consequently, during

cancer progression, tumour cells must rewire the regulatory and functional properties of their metabolic networks [94]. As cancer cells often retain a metabolic network similar to that present in their corresponding normal proliferating cells, the metabolic requirements are met by a combination of changes in the use of metabolic enzyme isoforms, which alter the uptake of nutrients such as glucose, increasing the excretion of waste products, such as lactate, and channelling of nutrients to biomass-generating pathways. Further, also mutations in oncogenes or tumour suppressor or metabolic enzymes genes and environmental conditions (hypoxia and inflammation) have been shown to have a role in cancer-related metabolic changes [95–97]. For these reasons, the concept of altered metabolism gained the status of a cancer hallmarks rather than only an indirect response to cell proliferation and survival signals [3].

1.3.1 Discovery of Otto Warburg

During the 1920s, Otto Warburg observed that tumours have an increased glucose uptake compared to surrounding tissue, and glucose is fermented to lactate even when oxygen is not limiting, hence the term 'aerobic glycolysis' or 'Warburg effect' [98]. This discovery led Warburg to hypothesize that the oxidative phosphorylation (OXPHOS) is impaired or damaged in cancer cells. However, this theory was largely contradicted by several studies showing that mitochondrial function was not diminished in most cancer cells, whereas higher rates of aerobic glycolysis in tumours have been repeatedly verified [99]. Only in 1980s the Warburg effect rekindled attention on cancer metabolism, with the introduction into clinic of 2-(^{18}F)-fluoro-2-deoxyD-glucose positron emission tomography (^{18}F-FDG-PET). This imaging technique, by using an analog of glucose, allows to image tumour by displaying areas in the body where there is a higher uptake of glucose [100]. For many cancer types, ^{18}F-FDG-PET coupled to CT has more than 90% sensitivity and specificity for the detection of primary and metastatic lesions [99]. Moreover, ^{18}F-FDG-PET is widely used in clinic for staging and restaging of cancer and several clinical studies focused on its usefulness to monitor the metabolic response to therapy (e.g.:breast and lung cancer) [101]. To date, the Warburg effect is still the most cited example concerning the occurrence of altered metabolism in tumours.

1.3.2 Glucose metabolism

Glucose is a major cellular energy resource and its metabolism allows cells to harness energy into the form of ATP. Once inside a cell, glycolysis occurs and glucose is converted into pyruvate with a net gain of two molecules of ATP and 2 molecules of NADH [99]. In the presence of oxygen (aerobic conditions), pyruvate is then transported in the mitochondria where it is oxidized to CO_2 and H_2O through the tricarboxylic acid (TCA) cycle and oxidative phosphorylation (OXPHOS), with a net yield of 32-34 molecules of ATP per molecule of glucose oxidized. When oxygen is limiting (anaerobic conditions), pyruvate undergoes fermentation and it is converted to lactate by lactate dehydrogenase (LDH) generating only 2 ATPs per molecule of glucose.

A main obstacle about understanding the propensity of cancer cells to rely on aerobic glycolysis is because aerobic glycolysis is a less efficient process over OXPHOS in terms of ATP production. An explanation is that glycolytic intermediates function as branching points between glycolysis and other pathways for macromolecule biosynthesis like nucleotide, lipids and protein. Thus, enhanced glycolysis supports the rapid growth of highly proliferating cells, providing the needed precursor for biosynthesis of macromolecules. Another explanation is that OXPHOS, even if producing higher number of ATPs, is a much slower process than lactate production from glucose, thus cannot counterbalance the needs of proliferating cells. It has been demonstrated that these two reactions can synthetize comparable amount of ATP in a given time [102]. Moreover, the transformation of pyruvate to lactate by LDH generate NAD^+, a reducing agent important for glycolysis. Despite how Warburg effect can benefit cancer is still a matter of debate [103], it is fairly clear that it might contribute to meet both bioenergetic and biosynthetic needs.

1.3.2.1 Regulation of glucose metabolism

Many glycolytic enzymes have been shown to be upregulated during tumorigenesis. For instance, the increased glucose uptake in cancer cells is associated with the upregulation of GLUTs. Among the 14 different isoforms currently described, GLUT1, GLUT2 and GLUT3 are found to be overexpressed in a variety of cancers [104] and GLUT1 expression in primary tumours has been correlated to poor prognosis [105]. Cancer cells usually promotes the irreversible step of phosphorylation and trapping of glucose inside the cells by the overexpression of HK2, in addition to HK1[106]. Moreover, the isoforms of LDH, especially

the isoform LDHA, is overexpressed in tumour cells, especially for its ability to recycle NAD^+ through lactate production.

The conversion of F6P to F1,6BP is regulated by PFK1, which activity is allosterically tightly regulated. Fructose-2,6-biphosphate (F2,6BP), generated by 6-phosphofructo-2-kinase/fructose-2,6-bisphosphatases (PFK2/FBPases), is an allosteric activator of PFK1 and counteract the allosteric inhibition exerted by ATP [107]. Another allosterically-activated enzyme is PKM2, which regulates the third committed step of glycolysis, by the action of F1,6BP and serine.

The key in renewing the interest on the Warburg effect derived from the discovery that mutation on the most prevalent proto-oncogene and tumour suppressor involved in cancer progression also drive reprogramming of metabolism. Regarding glucose metabolism, mutation in TP53, phosphatidylinositol 3-kinase (PI3K) signaling, Ras and Myc have been reported.

The tumour suppressor gene TP53 is mutated in most about 50% of all cancers. P53 is a transcription factor that can induce cell cycle arrest, senescence or apoptosis in response to cellular stress. p53 is involved in several step of glycolysis. For example, it limits glucose uptake by downregulating the expression of GLUT1 and GLUT4[108] or dampening the expression of HK2[109]. Another level of regulation by p53 is a direct activation of TP53-induced glycolysis and apoptosis regulator (TIGAR), which inhibits PFK1 to divert G6P into the oxidative pentose phosphate pathway, thus boosting the production of NADPH and overall reduction of reactive oxygen species[110]. In addition to inhibition of glucose transport inside the cell, p53 inhibits also the secretion of lactate by inhibiting the expression of monocarboxylate acid transporter 1 (MCT1)[111].

The PI3K/AKT/mTOR axis is a highly conserved pathway employed by cancer cells to respond to growth factor signals and among the most frequently deregulated in human cancers. Mutations that enhance this pathway occur by aberrant activation in growth factor receptors, loss of function of the tumour suppressor PTEN, acquisition of activating mutation in PIK3CA and amplification of the downstream effector AKT[112]. Activation of PI3K/AKT/mTOR pathway results in the upregulation of glucose transporters, like GLUT1 via AKT, therefore enabling increased uptake of glucose. In addition, AKT enhance the retaining of glucose by HK2- phosphorylating activity, and stimulate the activity of PFK1 [103]. An interest aspect of Akt derive from the fact that, whether is the mechanism of its activation, is sufficient to drive glycolysis and lactate production [113,114].

The *myc* family of genes (*c-myc, L-myc, s-myc*, and *N-myc*) encodes transcription factors that mainly target the expression of genes involved in growth and cell cycle entry and is frequently found amplified in tumours. Similar to other oncogenic transcription factors, c-Myc promotes aerobic glycolysis targeting many genes encoding glycolytic enzymes such as GLUT1 and LDHA [96].

The RAS oncogene has been widely characterized for its high transforming potential. The RAS family of genes, including KRAS, HRAS and NRAS, has a high rate of mutation in cancer, with KRAS being the most prevalent but still an undruggable target. RAS belong to a family of GTPase protein responsible for the transduction of extracellular signals from receptor tyrosine kinases to downstream effectors[115]. Activating mutations in RAS genes result in the constitutive GTP binding, and consequently the constitutive activation of several downstream effectors which promotes several malignant phenotype like proliferation, suppression of apoptosis and metabolic reprogramming among other [116]. Ras family act upstream of PI3K/AKT/mTOR pathway which in turn regulate the aerobic glycolysis. The main effects of Ras is that promotes the accumulation of the hypoxia inducible transcription factor HIF-1α, considered one of the master regulators of glycolysis, and the expression of several glucose transporter [117–120]. RAS regulates glycolysis also by increasing the activity of MYC and such interaction is an example of a cooperative mechanism between oncogenes to regulate metabolism[121].

1.3.3 Tumour cell metabolism and extracellular acidosis

Deregulated pH is a common feature of the solid tumour microenvironment, regardless the tissue of origin or the genetic background. In general, cancer cells display a decreased extracellular pH (pHe) (as low as 6.0 versus ~ 7.3-7.4 in normal cells), and an increased alkaline intracellular pH (pHi) (from 7.12 to 7.7 versus ~7 in normal cells) [122,123]. A combination of low perfusion of tumour mass, regional hypoxia and enhanced rates of glucose metabolism are commonly considered to contribute to the extracellular acidification [124].

1.3.3.1 Metabolic source of acidity in tumours

The phenomenon of extracellular acidosis during cancer progression is mainly associated with hypoxia due to its impact on energy metabolism [99,122]. The poor vascularization leads to an insufficient O_2 supply that results in a switch to a glycolytic O_2-independent

production of energy with a formation of high amount of lactate and protons. At the molecular level, hypoxia triggers the stabilization of hypoxia-inducible factor 1 α (HIF1-α) a master regulator of the Warburg Effect. For instance, HIF1- α directly regulates glycolysis by inducing the expression of glucose transporters (GLUT1 and GLUT3), thus enhancing the efficacy of glucose uptake and glycolytic enzyme like HK2 and PFK2 [125]. Of note, HIF1-α induces also the expression of pH-regulators like monocarboxylate transporter 4 (MCT4) and carbonic anhydrase 9 (CAIX) (see next section for more details). Overall, HIF-1 is a transcription factor which enhance the transcription of more than 60 genes that, beyond metabolism, regulates also angiogenesis and apoptosis. As reported previously, many other important oncogenes and tumour suppressor reinforce the acquisition of such a metabolic shift. Regardless the mechanism that guide to an upregulated glycolysis, this process results in the production of two molecules of pyruvate and two protons (H^+) and pyruvate is further converted to acid lactic by LDH. Lactate can be secreted from the cell by a class of protein called monocarboxylate transporters (MCTs) which co-transport one molecule of lactate and one proton H^+ [99]. Thus, the effect of lactate transport is the removal of one proton from the cell, which can acidify the extracellular space. Despite both *in vivo* and *in vitro* there is a good association between glucose uptake, as assessed by ^{18}F-FDG, and acidification, as measured by using pH-sensitive probes or Magnetic Resonance Imaging [126,127], glycolysis is not the only acid producing source in tumours. Indeed, models of LDH-A- and glycolysis-deficient tumours still results in extracellular acidification [128,129]. Another mechanism of proton production can be attributed to CO_2, the end-product of most human metabolic pathway. CO_2 is hydrated with H_2O into one molecule of HCO_3- and one H^+ by carbonic anhydrases (CA), contributing to acid production. However, the growth of the tumour mass occurs with a disorganized vasculature that impede both a good perfusion and inefficient clearance of the locally produced CO_2 and H^+ that normally would be buffered into the bloodstream [124,130].

1.3.3.2 pH regulation in tumours

Regardless the sources, excessively produced H^+ must be removed from the cells. H^+ are the smallest and reactive species present in living organism and their concentration, thus the resulting pH, might affect protein structure and enzyme activity and consequently disrupt any cellular processes (metabolism, protein synthesis, proliferation and apoptosis). To avoid such perturbation in pH homeostasis, cancer cells employ various net acid

extrusion mechanism such as the sodium–hydrogen (Na^+/H^+) exchanger, in particular the isoform NHE-1, the vacuolar-type H^+-ATPase (V-ATPase), the monocarboxylate transporters (MCTs), and the carbonic anhydrase (CA)[131].

Among the several NHE described, the most relevant isoform in the contest of pH-regulation and cancer development is NHE1, a transmembrane protein, ubiquitously expressed, which mediate an active acid extrusion by exchanging extracellular Na^+ for intracellular protons [131]. Its expression is often localized to the edge of invading cells and its depletion causes drastic loss of tumorigenicity, underlying the importance of pH regulating system in cancer progression [132].

MCTs are part of a family of plasma membrane transporter proteins, known also as SLC16 solute carrier family [133]. Four isoforms of this family (MCT1-4) catalyse the proton-linked transmembrane transport of monocarboxylates such as L-lactate, pyruvate and ketone bodies [134]. Marked overexpression of MCT1 and/or MCT4 is a hallmark of several cancer types and increased levels of these transporters are associated with poor outcome. For instance, upregulation of MCT1 and MCT4 have been detected in lung, breast and colorectal cancer [125,135].

V-ATPase is a member of the ATPases family, which couple ATP synthesis or hydrolysis with the extrusion of an ions across the membrane. V-ATPases are expressed on the plasma membrane of human cancer cells and involved in the H+ pumping. They contribute to tumour invasion and growth, and several report claim their involvement in multidrug resistance phenotype in cancer cells [136]. V-ATPases are found overexpressed in several cancer types such as breast, NSCLC and glioblastoma.

Carbonic anhydrases are a family of enzyme responsible of the reversible hydration of CO_2 to HCO_3- and H^+. This family comprises 16 members and the isoform CAIX has emerged as one of the most relevant. CAIX expression is mainly induced by hypoxia through the fine regulation of HIF1-α. Depletion of CAIX resulted in intracellular acidosis and reduced tumour growth [137,138]. In addition, CAIX expression has been widely correlated with poor outcome in several human cancers [136].

1.3.3.3 Pathogenic effect of tumour acidosis

This reversed pH gradient across the plasma membrane occurs early in carcinogenesis [132] and increases with the progression of cancer by promoting proliferation, resistance to apoptosis, metabolic reprogramming, migration, invasion and anchorage-independent

growth [124,130,139]. Thus, the extracellular acidification feature is not only a mere consequence of tumour metabolism, but it is important for cancer cells to gain selective advantages and a more aggressive phenotype [123]. In this regard, concentration of ions follows a gradient from tumour into adjacent normal tissue, enabling tissue remodelling at the tumour and stroma interface. Indeed, the extracellular acidification promotes the expression of cathepsins and metalloproteinases, which in turn drives the degradation of the extracellular matrix [139], and induces the release of pro-angiogenic factors (VEGF and IL-8), that triggers the formation of new blood vessel favouring tumour cell dissemination [140,141]. Normal cells are usually sensitive to acidosis induced death, while cancer cells have adapted to this adverse condition by developing mechanism of resistance to various cytotoxic factors. The extracellular acidification of cancer cells has been also associated with a mechanism of chemoresistance ("ion" trapping) as the entry of a drug into a cell depends on both concentrations and pH. There is a group of drugs which behave as weak bases (e.g.: doxorubicin) that in an acidic microenvironment are protonated. The resulting charged form has a strongly reduced membrane permeability and subsequently the cellular uptake is decreased. Conversely, drugs that behave like weak bases, cross the plasma membrane and accumulate into acidic organelles (lysosomes, endosomes, secretory vesicles) [142]. Finally, tumour acidosis and also secretion of lactate are believed to exert an immunosuppressive effect by inducing anergy in T-cells [143].

2. AIM OF THE STUDY

CTCs are cancer cells disseminated into the blood from primary or metastatic sites [15]. Evaluation of CTCs isolated from the peripheral blood has demonstrated clinical validity as a prognostic and predictive tool based on enumeration, but has failed to demonstrate its clinical utility [17].

To date, CellSearch® platform is the only FDA-approved platform for CTC detection and enriches epithelial cells targeting EpCAM-positive cells. Using only EpCAM to isolate CTCs is considered one of the major limitations of this technology as EpCAM can be downregulated during the EMT process and, consequently, CellSearch® might fail in the identification of a subpopulation of cells. Hence, there is a need to develop alternative and/or complementary platforms for the characterization of CTCs to exploit their diagnostic, prognostic and biological roles.

Deregulated metabolism has been recently listed as a hallmark of cancer [3]. Most cancer cells have an increased glucose uptake and lactate production, which is released into the extracellular space causing the acidification of the tumour microenvironment. Even if such metabolic alterations are well known, they have never been used to detect CTCs.

Our group has recently developed a method to detect cells with an altered metabolism, based on the differential extracellular acidification rate between normal and cancer cells. This assay exploits a droplet microfluidic technology, which allows to compartmentalize single-cell into a droplet and detect hypermetabolic cells by pH measurements of the extracellular space.

On these grounds, the aim of this study was to evaluate the single-cell metabolism-based method for detecting CTCs in a clinical setting. In more details, a reproducible methodology to process blood samples from cancer patients was established and validated. Then, the clinical performance of the metabolism-based assay was investigated by a comparison with the CellSearch, as the gold standard for CTC enumeration in MBC. Finally, the presence of neoplastic cells among the detected hypermetabolic cells was evaluated.

3. MATERIAL AND METHODS

3.1 Microfluidic platform

3.1.1 Device fabrication

In this work, one microfluidic device was employed for droplet generation and/or droplet fluorescence data acquisition, and a second one for fluorescence activated sorting of droplets. Each device was made of PDMS bonded to glass surface using soft lithography techniques [59]. Twenty-five µm thick layer of SU8-2025 were spun on silicon wafer, baked, exposed through transparency mask, baked again and developed according to manufacturer instructions (MicroChem corp., MA, USA). Sylgard 184 (PDMS) prepolymer and crosslinking agent (Dow Corning) were mixed at a mass ratio of 10:1 (w/w); a mixture was poured onto a master, degassed and cured at 65°C for at least 2h. The replica was detached from master and reservoirs were bored using a blunt hypodermic needle. A PDMS replica was washed in ethanol and blow dried with nitrogen. A clean glass slide and a clean PDMS replica were treated with oxygen plasma and bonded. The emulsification device was silanized with 5% (Tridecafluoro-1,1,2,2-Tetrahydrooctyl)-1-Trichlorosilane (Sigma-Aldrich) in FC-40 (3M) perfluoro silane, fluorinated oil, which was introduced into microfluidic channels (enough to completely wet whole microfluidic network) and then the device was kept at 95°C for at least 30 min. The sorting device was instead silanized with two silanization agents - [perfluoro silane] and 1% of 11-bromo-undecyl-dimethyl-chlorosilane in cyclohexane [Br silane] for 10 min. Perfluoro silane] was injected in oil waste outlet at 150µL/h, and simultaneously [Br silane] was injected into the water outlet at 500 µL/h. Afterwards whole network was flushed with filtered HFE7500 and nitrogen, last two steps were repeated 3 times. Finally, device was kept at 95°C for at least 30 min. Finally, device was kept at 95°C for at least 30 min. Subsequently, the electrodes were casted by melting 51In/32.5Bi/16.5Sn low temperature solder into the corresponding microfluidic channels. While the solder was still liquid, short pieces of electrical wires were introduced to serve as electrical connection.

3.1.2 Optical setup

The optical setup for measuring droplet fluorescence (Figure 3D) consisted of an Olympus IX70 inverted fluorescence microscope. A 25mW, 405 nm laser beam was expanded (2x) and focused down with a cylindrical lens crossing orthogonally the microfluidic channel. Fluorescence signal emitted from droplets was captured by a 40x objective (Olympus

LUCPlanFLN, 40x/0.60), split with dichroic filter (DLP555, Semrock) and detected through bandpass filters (579/34; 630/38, 494/20 and 435/20) by Photo Multiplier Tubes (PMTs) (H957-15, Hamamatsu). Signal went through a transimpedance amplifier with 1V/uA gain and detected by the acquisition system (National Instruments cRIO-9024, analog input module NI9223) with a 10 μsec scan rate.

3.1.3 Design of microfluidic devices

The design of the emulsification and data acquisition microfluidic device is reported in Figure 2.

The emulsification device contained: i) two inlets, one for cell suspension (also referred to as aqueous phase) and the other one for carrier oil phase (or continuous phase); ii) one outlet for droplet collection; iii) a 20 μm wide flow-focusing junction and iv) passive filters at the inlets to prevent channels from clogging.

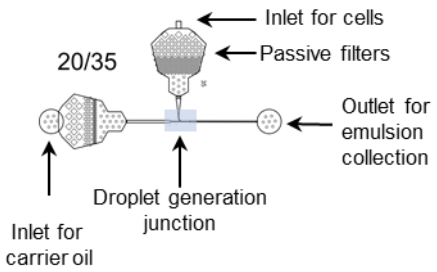

Figure 2. Schematic overview of the microfluidic device employed for droplet generation and data fluorescence acquisition.

3.1.4 Droplet generation and encapsulation of cells

The emulsification device was used to generate droplets. This device has a flow-focusing junction, where the aqueous phase (cell suspension) and carrier oil stream meet, and droplet generation occurs (forming a water-in-oil emulsion). To stabilize droplets against coalescence, 1% (w/w) 8-fluorosurfactant (RAN biotechnologies) was dissolved in HFE-7500 (3M) Novec (Fluorochem Ltd., UK) fluorinated carrier oil.

Cell suspension was loaded into a low-binding tip (Standt) connected to a 2.5 ml syringe via Polytetrafluoroethylene (PTFE) tube (0.56 mm × 1.07 mm internal/external diameter; Fisher Bioblock) and pre-filled with HFE-7500 (3M) Novec (Fluorochem Ltd., UK) fluorinated oil to fulfil dead volumes and pumped into the microfluidic device at 300 μl/h. The carrier oil phase was loaded into another syringe (Hamilton) and pumped in at 600 μl/h. These streams meet at the 20 μm wide flow-focusing junction, where the droplet

generation occurs as the cell suspension stream broke up into 15 pl droplets. The resulting emulsion flowed off-chip through PTFE tubing (0.56 mm × 1.07 mm internal/external diameter; Fisher Bioblock) connected to the outlet of the device and collected into 1.5 ml vial placed on an ice-cold rack (IsoTherm System, Eppendorf). The vial containing droplets was incubated for the desired incubation time at 37°C in a humidified incubator with 5% CO_2. After incubation, droplets were immediately cooled by replacing the vial on the ice-cold rack and reinjected into the required microfluidic device for subsequent analysis.

3.1.5 Droplet screening

Droplets were reinjected into the emulsion device through PTFE tubing (0.56 mm × 1.07 mm internal/external diameter; Fisher Bioblock) connected to a 2.5 ml syringe (Hamilton) previously filled with HFE7500 oil at a flow rate of 100 µl/h. Droplets were spaced out at the flow focusing-junction by the injection of carrier oil at a flow rate of 200 µl/h. When the system had stabilized, the fluorescence of each flowing droplets was acquired by the optical set up as above described.

3.1.6 Data fluorescence acquisition and control system

To record droplet fluorescence intensities and trigger the camera to capture images of droplet with predefined fluorescence intensities and the electrodes, a National Instruments FPGA data acquisition card (cRIO-9024, analog input module NI9223) driven by a LabVIEW custom software were used. The data acquisition system had a 10 µsec scan rate. The signal output voltage of each droplet is recorded and processed in real time by a Field Programmable Gate Array (FPGA) card and select droplets with a fluorescence intensity over a set threshold and size (a parameter determined by the residence time of the droplet in the laser spot and used to exclude from the analysis droplets that coalesced or are too small). These features are used in selecting whether the droplets should be capture by pictures or sorted. When PMT voltage exceeds a defined threshold and the droplet size falls in the expected range, the camera is triggered. In the case of sorting, a high-voltage train of pulses, consisting in a square wave of 30 Hz and 1 kV peak-to-peak amplitude, was applied to the electrodes. A user interface allows the operator to interact with the instrument and tune various parameters such as the fluorescence threshold for droplet imaging and sorting and activation of filters for droplet size. Data are transferred from the FPGA to the CPU providing a record of images and raw tracks for each run. A written-in-house LabVIEW software allows the operator to access to the picture gallery, verify simultaneously the

content of the droplet and the raw track, and a trained operator classifies the events according to the defined criteria.

Liquids were pumped into the microfluidic device by using neMESYS (Cetoni) low-pressure syringe pump and gastight syringes (Hamilton). These were connected to the microfluidic device using syringe connector luer lock and PTFE tubing with an internal diameter of 0.56 mm and an external diameter of 1.07 mm (Fisher Bioblock Scientific).

3.2 pH-assay for extracellular acidification measurements

The pH-sensitive fluorescent dye SNARF-5F (Invitrogen) was used to measure the pH of each droplet. SNARF-5F respond to pH variation undergoing a wavelength shift in the emission spectra (Figure 3E). Such pH-dependent shifts allow the ratio of the fluorescence intensities from the dye at two emission wavelengths (580nm and 630nm) to be used for quantitative determination of pH. For each droplet the ratio of emitted fluorescence intensities at 580 and 630 nm (580/630 ratio) of SNARF-5F is calculated in real time. As the pH is more acidic, SNARF-5F fluorescence increases at 580 nm while decreases at 630nm (Figure 3E). As a result, when the pH inside a droplet decreases below pH 7.4, an increase in the 580/630 ratio over 1 is observed. To calibrate the system, Joklik's EMEM medium titrated at different pH (7.4, 7, 6.5, 6, 5.5 and 5) was added with 4 µM SNARF-5F, emulsified and droplets screened for fluorescence. The 580/630nm ratio were calculated for each pH and plotted against the respective pH, which allowed constructing a calibration curve (Figure 4B).

3.3 Cell lines

The breast cancer cell lines MDA-MB-231 and MCF7, were obtained from the American Type Culture Collection and cultured in DMEM medium (Sigma) supplemented with 10% FBS. The ovarian cancer cell lines IGROV-1 and OC316 were grown in complete RPMI 1640 medium (Sigma) supplemented with 10% FBS, 10 mm Hepes (Gibco) and 1% Na-pyruvate (Sigma). All cell lines were grown in a humidified atmosphere at 37 °C and 5% CO_2. All cell lines were validated for short tandem repeat profiling.

3.4 Study design

A pilot study trial was conducted to compare the metabolism-based assay and the CellSearch® system for CTC enumeration. A total of 31 patients with progressive and measurable MBC, at the start of a new systemic therapy, without limits to number and kind

of previous therapies (hormone therapy, chemotherapy, targeted therapy) were included. All patients had an Eastern Cooperative Oncology Group performance status (ECOG PS) score ≤ 2.

Before starting a new therapy, patient underwent baseline blood drawn for CTC evaluation and standard clinical studies. Another blood sample was collected after 3-4 weeks the start of the therapy (follow-up). Revaluation of disease status were conducted depending on the type of treatment the patient received and the schedule of the therapy. Standard Response Evaluation Criteria In Solid Tumours (RECIST) criteria were used to determine patients' responses to treatment. The study was conducted at the IRCCS-CRO Aviano-National Cancer Institute and approved by our Institutional Review Board. Informed and written consent was obtained from all patients and healthy donors before their enrolment, and their clinicopathological information was recorded.

3.5 CTC detection by the metabolism-based assay

Blood samples were drawn into K_2-EDTA Vacutainer tubes (Beckton Dickinson) and maintained at room temperature. For each sample, 2.5 ml of blood were analysed within 2 hours after collection. Red blood cells (RBC) were lysed with a 1X FACS lysing solution (BD PharmLyse) and centrifuged at 200g for 5 min. Thereafter, the nucleated fraction was depleted of CD45-positive WBCs and residual RBCs using CD45 and Glycophorin A microbeads (Miltenyi Biotec), respectively, and LD separation columns in a MACS MIDI separator (Miltenyi Biotec), according to the manufacturer's instructions. The unlabelled cells were recovered, centrifuged at 300g for 10 min and stained with anti-CD45 (BD Horizon Brilliant™ Violet 480, dilution 1:100) and anti-EpCAM (BD Horizon Brilliant™ Violet 421, dilution 1:100) for 25 min at room temperature. After washing the sample with PBS-BSA 0.5%, cells were resuspended in 50 μl of the unbuffered Joklik's modified EMEM culture medium (Sigma) containing 2mM EDTA, 0.1% BSA, 15% Optiprep and 4mM of the fluorescent pH indicator SNARF-5F (Thermo Fisher Scientific). Then, cells were single-cell encapsulated in monodispersed droplets using the droplet microfluidic platform as described in the microfluidc platform section. The emulsion was collected and incubated at 37^{o} C for 30 min and then reinjected into the microfluidic channel for fluorescent reading of pH, CD45 and EpCAM expression, and the acquisition of bright-field imaging of each positive event. Positive events were defined as droplet containing a

$CD45^-$, $EpCAM^+$ or –, and $Acid^+$ cell. The number of CTCs was then normalized to 7.5mL to be comparable to that observed with the CellSearch.

3.6 CTC detection by CellSearch

CTC isolation and enumeration were performed using the CellSearch® system. Blood samples were drawn into 10 mL CellSave Preservative Tubes (Menarini), which contains a proprietary fixing preservative, and maintained at room temperature. Blood samples were sent to the IRCCS-Istituto Oncologico Veneto (IOV) and processed within 96 h after collection by trained personnel. For each sample, 7.5 ml of blood were transferred into a specific 15 ml conical tube, mixed with 6.5 ml of CellSearch dilution buffer and centrifuged at 800g for 10 min without brake. The tube was loaded into the CellTracks AutoPrep system, a semiautomated instrument used for the preparation of the sample with the CellSearch Epithelial Cell Kit. In brief, the instrument aspirates the plasma and adds ferrofluid particles coated with anti-EpCAM antibodies and a capture enhancement reagent. After incubation and magnetic separation, unbounded cells are removed. Ferrofluid-labelled cells are re-suspended in a buffer, permeabilized and stained with phycoerythrin-conjugated antibodies directed against cytokeratin (CK) 8, 18 and 19 to specifically identify epithelial cells, an antibody allophycocyanin-conjugated against CD45 to identify remaining WBC and the nuclear dye 4,6-diamidino-2-phenylindole (DAPI) to label the cell nucleus. To quantify the fraction of apoptotic CTCs, anti-M30 monoclonal antibody marked in FITC was integrated in the assay for recognizing a neoepitope in cytokeratin 18 (CK18) that becomes available at a caspase cleavage event during apoptosis and is not detectable in viable epithelial cells. The sample is then washed and automatically transferred to a cartridge, which sits in a magnetic field (Magnest®) and allows cells to migrate to the analytical glass surface. The cartridge is scanned for each individual fluorochrome by using a semiautomated fluorescent microscope, named CellTracks Analyzer II. The software selects and presents all captured images that contain objects fitting the predefined criteria and a trained operator classifies the events according to the CellSearch® CTC definition. According to the guidelines of the CellSearch® method, a cell is classified as CTC when is positive for the phycoerythrin-cytokeratin and DAPI staining and negative for allophycocyanin-CD45 staining. CTCs must have a size of at least 4 μm, a round to oval morphology and a nucleus surrounded by cytoplasm for 50% of its

surface. All evaluations were performed without knowledge of the clinical status of the patients.

3.7 DNA extraction, purification and quantification

DNA extraction from CTC was performed using the automated Maxwell 16 Instrument with the Maxwell® RSC ccfDNA Plasma Kit (Promega), following the manufacturer's instructions. DNA was quantified by using QuantiFluor® dsDNA System (Promega), according to the manufacturer's protocol.

3.8 DNA mutation detection

DNA extracted from sorted cells was analysed for the hot spot drug resistance point mutations of ESR1 (Y537N, Y537S, D538G, L536R) using droplet digital PCR. ddPCR was performed using a Droplet Digital PCR XQ200 system (Bio-Rad Laboratories).
Briefly, about 5ng of DNA was added to a 20μL PCR mixture containing 10μL ddPCR Supermix for probes (No dUTP; Bio-Rad Laboratories), 900nM target–specific PCR primers, 250nM mutant–specific (FAM) and wild-Type-specific (HEX) probes. 20μL PCR mixture and 70μL Droplet generation oil for Probes (Bio-Rad Laboratories) were mixed and droplet generation was carried out according to the manufacturer's manual. The droplet emulsion was thermally cycled in the following conditions: 95 °C for 4 min (1 cycle), 94 °C for 30s (ramp rate 75%) and 58° C for 1 min (40 cycles), and infinite hold at 4°C. Prior to sample testing, thermal gradient experiments were performed to determine the optimal amplification conditions. Samples were analysed as technical duplicates and positive WT controls were used in all assays performed, in order to verify assay performance and facilitate the analysis of fluorescence values. Droplet fluorescence data and quantification of template abundance were analysed with the QuantaSoft software (Bio-Rad Laboratories).

3.9 Statistical analysis

Data were analysed using GraphPad Prism 6 (version 2.6). Patient and clinical characteristics were presented as frequency and percentage, median and range, mean and standard deviation (SD), as appropriate. Comparison of median between groups were performed by Mann-Whitney test and groups were compared using the Wilcoxon rank test. PFS and OS (time elapsed from enrolment to disease progression and death from any cause, respectively) were determined by Kaplan–Meier plots, with data being censored at last follow-up if progression or death had not occurred. Gehan-Breslow-Wilcoxon test were

used to compare the survival curves by CTC detection groups. $p < 0.05$ was considered significant.

4. RESULTS

4.1 Working principle and validation of the detection platform

4.1.1 Description of the platform for pH measurement

Encapsulation of cells into droplets is an effective analytical tool as metabolites released from cells remain trapped in the picoliter (pL) droplets. Thus, secreted molecules quickly reach detectable concentration because of the small droplet volume, enabling sensitive measurement on single cells that are typically not feasible via bulk cellular measurement [144–146].

A feature of cancer cells is their altered metabolism, typically associated with an increased glucose consumption, which in turn involves a high production and secretion of proton H^+. The increasing concentration of H^+ leads to the acidification of the extracellular microenvironment, and this correspond to a measurable decrease in the pH value.

To investigate the potential utility of enumerating CTCs with an altered metabolism in clinical samples from cancer patients, our group developed a droplet microfluidic-based assay for the pH measurement at single-cell level [147]. Figure 3 outlines the overall strategy. Briefly, cells to be tested for the extracellular acidification level were encapsulated into 15 pL droplets together with a ratiometric pH sensitive dye (SNARF-5F) for pH readout (Figure 3A). During in-drop incubation, because of the cellular metabolic activity, each cell released a certain quantity of H+ altering the pH of the droplet-containing cells environment (Figure 3B). Droplets were then reinjected into the device and screened for fluorescence pH measurement by the optical setup (Figure 3C-E). As pH is lowered, SNARF-5F undergoes a wavelength shift in the emission spectra, allowing to determine the exact pH of the droplet by comparing the fluorescence peaks at two wavelengths (ratio 580/630 nm) (Figure 3E). As the optical setup has comprehensively four fluorescence channels, two more fluorophores can also be detected simultaneously with SNARF-5F. In this work they were exploited to identify EpCAM and CD45 expression. Finally, the content of each droplet with a fluorescence signal over an operator-dependent threshold could be imaged, thus providing an additional verification of the content (Figure 3D) and quantified.

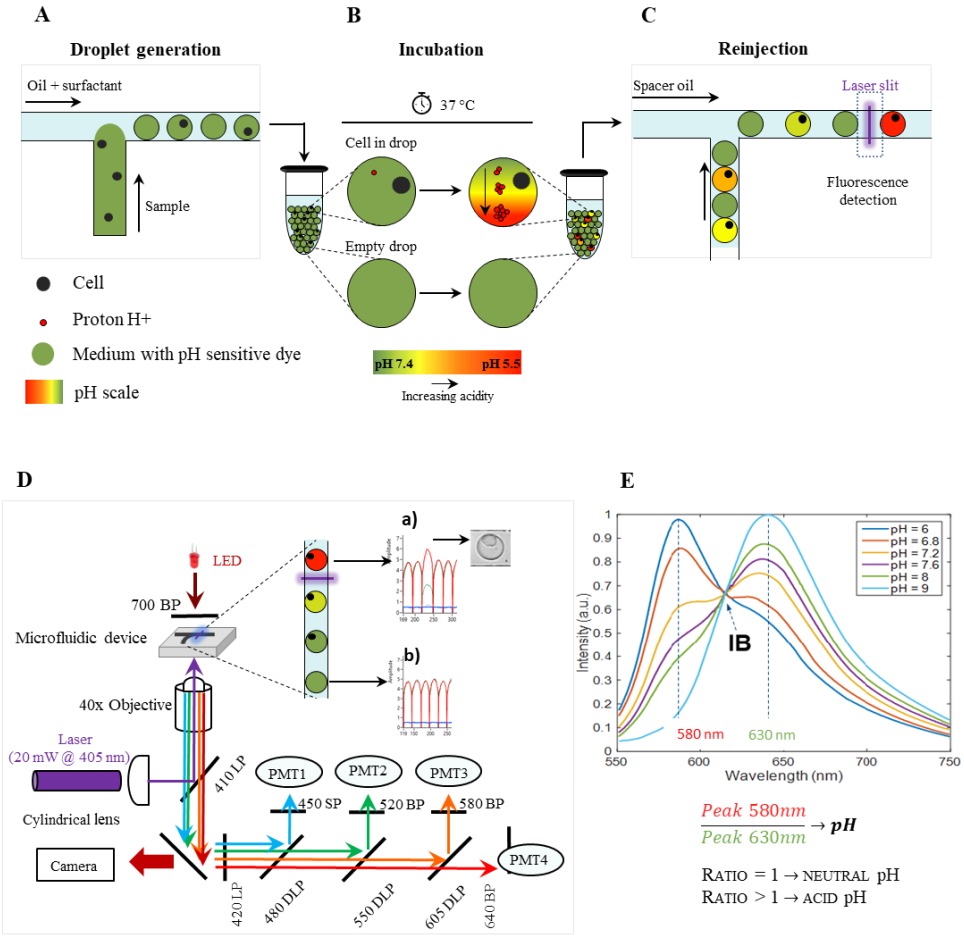

Figure 3. Schematic overview of the droplet microfluidic single-cell assay for determination of the extracellular pH. A) Single cells were encapsulated into picoliter droplets together with an extracellular pH-sensitive dye (SNARF-5F); B) During in-drop incubation, single cell secreted a certain quantity of proton H^+ which leads to a decrease of the pH value (i.e.: acidification of the droplet environment) C) The water-in-oil emulsion was reinjected into a second microfluidic device and droplets screened for fluorescence by the optical setup. D) Schematic overview of the optical set-up: laser light (405 nm) was emitted from the laser, shaped into a laser line through cylindrical lens and transmitted through a dichroic mirror to the microscope. Fluorescence signals emitted from droplets were captured by a 40x objective, split with dichroic filters, and then reflected by dichroic filter to photomultipliers (PMT) (solid line represents dichroic filters; DLP = dichroic long pass; SP = short pass). Insertions: a) representative image of an in-drop cell with the corresponding fluorescence spectrum from which a decrease of fluorescence intensity at 630nm (green line) and an increase in 580nm (red line) can be observed, as expected from an acidic droplet; b) empty droplet showing no change in the pH, i.e. in the ratio of SNARF-5F fluorescent intensity at 580 and 630nm; E) Fluorescence emission spectra of SNARF-5F showing the spectral pH-dependent shift at 580nm and 630nm.

The droplet microfluidic device used for droplet generation and droplet fluorescence data acquisition is schematically illustrated in Figure 2. The microfluidic device was made of PDMS bonded to glass surface using standard protocols [59]. In this set up, two microchannels intersect to form a flow-focusing junction where the two immiscible fluid (i.e. the aqueous cell suspension and the oil added with surfactant) meet generating monodispersed droplets along with the encapsulation of cells. As previously demonstrated [148], this occurs as the liquids flow into channel at a rate in which the shear force at the fluid interface is sufficiently large to cause the oil phase to break up the aqueous, i.e.: the cell suspension, into discrete droplets. Droplets are thermodynamically metastable then a surfactant is added to the oil for their stabilization. The use of fluorinated oil has a good solubility for oxygen and biocompatibility, as previously shown [144].

4.1.4 SNARF-5F allows to discriminate population of droplets with different pH

The ratiometric pH indicator SNARF-5F allows pH measurement and it has been previously used to detect pH both *in vitro* and *in vivo* [126,149].

To obtain a calibration curve to convert the 580/630 nm ratio value into pH, an unbuffered culture medium, Joklik's modified EMEM, was titrated at various pH between 7.4 and 5, emulsified, and then analysed by the optical setup. Once the PMTs gain were set to have a ratio 580/630 nm equal to ratio 1 for the neutral pH of 7.4 as a reference, the fluorescence signals of droplets containing medium at decreasing pH were recorded (this setting was used as well for other experiments described in this work). As shown in Figure 4A, there is an inverse correlation between 580/630nm ratio and the value of pH. The mean average of fluorescent ratio intensities was plotted in function of known pH value and a sigmoidal fitting performed to obtain a calibration curve (Figure 4B). The system was calibrated periodically. Finally, the ability of the system to discriminate the presence of different population of acidic droplets was further confirmed by mixing droplet generated separately and containing medium at different pH. As shown in Figure 4C, the system was able to clearly distinguish each population of droplets.

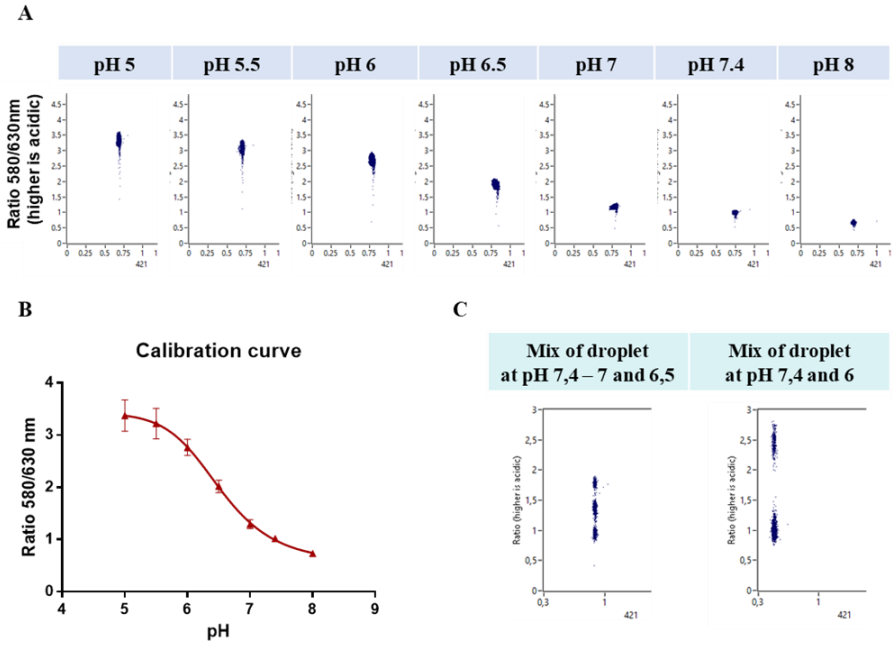

Figure 4. Calibration of SNARF-5F. A) Representative dot plots showing the decreasing SNARF-5F 580/630nm ratio mean fluoresce intensity of droplets containing buffers at increasing pH; B) Calibration curve of SNARF-5F. Ratio of 580 and 630 nm SNARF-5F fluoresce intensity was plotted for each respective pH and a sigmoidal fit was performed to obtain the represented calibration curve. C) Droplets generated with buffer at known pH value were mixed and then the data fluorescence recorded.

4.1.5 Decreasing the rate of false positive events

Our previous work reported that few false positive droplets could be imaged. These false positive events corresponded to acidic droplet containing material like cell debris, which also could impair the step of emulsion by clogging the junction, or empty droplets. Since the described method had to be applied for CTC detection, which are commonly rare events, it was desirable to decrease at maximum the occurrence of the aforesaid false positive events.

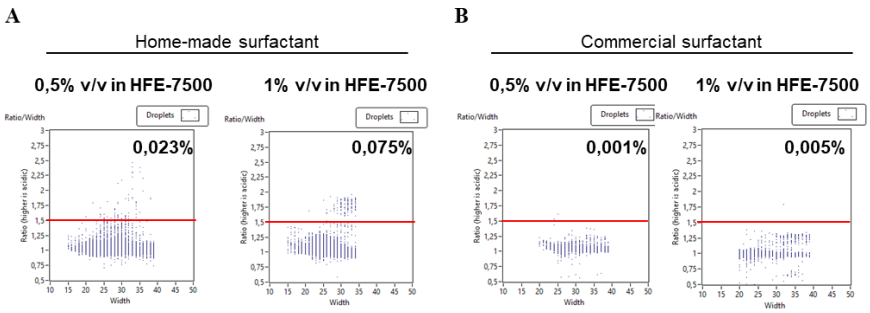

Figure 5. Rate of false positive events recorded on 200000 empty droplets generated with oil HFE-7500 added with increasing concentration of A) a home-made surfactant and B) a commercially available one.

First, to prevent clogging of the junction, passive filters have been incorporated upstream of the nozzle. Then, the effect of increasing the concentration of a home-made synthetized surfactant were explored. Figure 5A reports representative dot plots which highlight that an increase in surfactant concentration from 0.5% to 1% corresponded to an increase of false positive from 0.023% to 0.075%. Considering that this phenomenon was stochastic and varied from batch to batch, a commercially available surfactant was finally tested. As shown in Figure 5B, the number of false positive events significantly decreased to 0.001%.

4.1.5 Determination of the droplet volume size for pH measurement in patient samples

The size of droplets is determined by the ratio of the volumetric rates of liquid flow, which are tightly controlled by using a low-pressure syringe pump, gastight syringes and PFTE tubes connected to the device. To determine the optimal size of droplet to distinguish WBCs from CTCs in patient samples, a determination of ratio as a function of droplet size was performed for both MDA-MB-231 and WBCs. Table 3 summarises the flow rates employed, and the corresponding droplet volumes obtained. Since the proton release of the investigated cells is assumed to be constant, the resulting pH, that is the concentration of H^+, is dependent from the volume where they are detect. As expected, the mean ratio fluorescence intensities of both MDA-MB-231 and WBC decreased as droplet volume increased, confirming that the ratiometric nature of SNARF-5F as a dye that shifts its wavelength upon the concentration of protons can be exploited also in the system employed in this study for pH measurements (Figure 6). Since droplets of smaller volumes allowed both a good separation between cancer cells and WBCs within a wide range of pH values and allowed the generation of monodispersed droplets, the flow rate of 600µl/h and 300µl/h for oil and cell suspension, respectively, was adopted for this study.

Oil phase (ml/h)	Cell suspension (ml/h)	Volume (pl)
0,7	0,3	13
0,6	0,3	15
0,4	0,3	18
0,25	0,3	25
2,5	0,5	42*
1,5	0,5	63*
0,7	0,1	78*

* Commercially available microfluidic chips (with a different architecture respect to that normally employed in this work) were used to obtain this droplet volume.

Table 3. Table summarizing the volumetric flow rates for both oil and cell suspension phase and the correspond droplet volumes obtained.

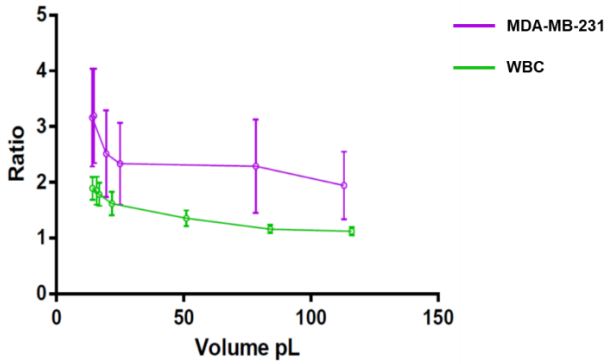

Figure 6. This graph reports the mean±S.D. fluorescence of 580/630 nm ratio in function of varying droplet volume size for MDA-MB-231 cell lines (violet line) and WBCs (green line).

In accordance with previous studies [144,145], the process of encapsulating cells is random and follows a Poisson distribution curve. As a result, most droplets are empty of cells and the droplet occupancy (i.e. the number of cells inside a droplet) can be adjusted by varying the cell suspension concentration. In this study, the generation of 15 pL droplets using a cell density of $1x10^6$ cells/ml, which is much higher than that expected after the processing of blood sample for CTC detection, resulted in an encapsulation efficiency of approximatively 2% cell-containing droplets, 94% of which contained a single cell. Further, since empty droplets account for at least the 98% of total droplets and they are expected to contain only the unbuffered medium at the neutral pH of 7.4, such population was used as an internal reference to set the analysis of pH measurements.

4.1.6 Effects of room temperature on the extracellular acidification level

To assess whether the room temperature could introduce bias on pH measurements, that have to be clearly avoided in the light to apply this method for rare cells detection in clinical samples from cancer patients, MDA-MB-231 and WBC in-drop cells were screened after 10 min of incubation, with or without a temperature control system, at several time point. Overall, after incubation, the effects of temperature were assessed every 10 min over a period of 40 min, which approximately corresponds to the time required for the acquisition of a clinical sample.

The rise of the mean ratio of MDA-MD-231 and WBCs respect to that recorded immediately after incubation, highlighted that protons were released over time when the sample was left at room temperature (Figure 7A and B, left panels). In particular, such effect was more evident for the breast cancer cells, suggesting again that cancer cells have a higher proton release rate respect to that observed for WBCs. To lower the cellular metabolic activity, refrigerated solutions and a cooling system which permits to maintain

the sample at a constant temperature of 4°C were employed during the step of generation and collection of the emulsion, immediately after the incubation, and during reinjection. This resulted in an unchanged value of pH compared to that recorded immediately after incubation (Figure 7A and B, right panels**)**. Overall, these results highlighted the need to adopt the described temperature control strategy.

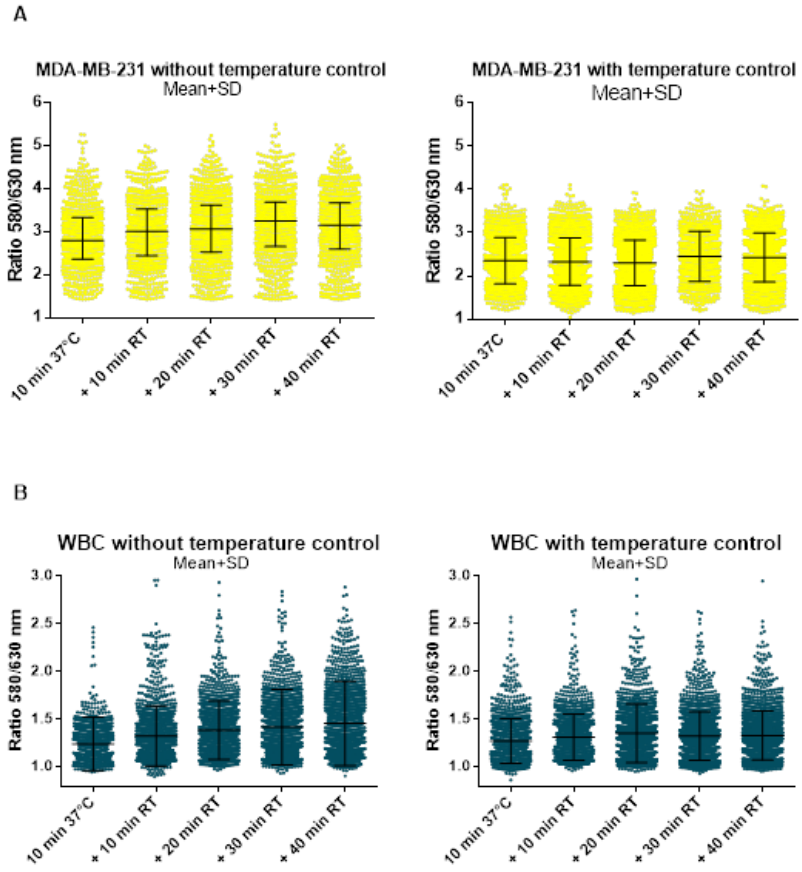

Figure 7. Evaluation of the room temperature effects on the single-cell metabolism-based assay. Both MDA-MB-231 and WBCs were emulsified with (A) or without (B) a temperature control approach. After 10 min of incubation, each emulsion was aliquoted in 5 samples and left at room temperature or on ice for 0, 10, 20, 30 or 40 min. The graph reports the mean average ± S.D. fluorescence intensities of 580/630nm ratio measured each time point of incubation.

4.1.4 Glucose effect on the extracellular acidification rate

It has been widely described that the presence of glucose in solution enhances cellular metabolism in glycolytic cancer cells, in contrast to what observed in normal or non-metastatic cancer cells. Thus, to further confirm that the extracellular acidification observed was a consequence of an altered metabolism, MDA-MB-231 and WBC were emulsified in the presence of increasing concentrations of glucose (0mM, 5mM and 10mM). As

expected, the breast cancer cells showed a decreased pH after incubation, which was even more evident with the increase of glucose concentration. On the other side, a significant drop in the acidification of droplets containing WBC was observed only at 5mM of glucose, whereas no significant changes were monitored with increasing concentrations (Figure 8).

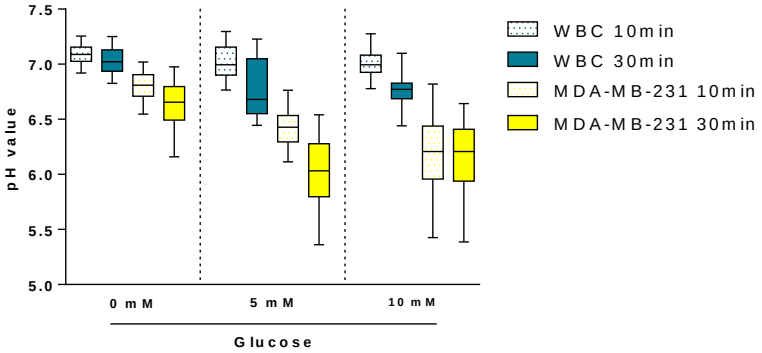

Figure 8. Extracellular acidification measured for MDA-MB-231 and WBCs in function of increasing concentration of glucose (0-5-10 mM) measured both after 10 and 30 min of incubation at 37°C.

The extracellular acidification of two ovarian cancer cell lines, namely OC316 and IGROV-1, which are described as cells with a high and low glycolytic phenotype, respectively, were assessed. In accordance with the previous finding that OC316 has a higher level of extracellular acidification rate respect to IGROV1[150], as detected by the Seahorse flux analyser, our method recorded lower mean value of pH for the OC316 respect to IGROV-1 (Figure 9). Thus, our method was able to discriminate among cells with distinct feature of glucose consumption.

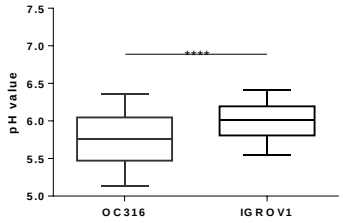

Figure 9. The extracellular acidification level detected for the highly glycolytic OC316 was significantly lower than the low glycolytic IGROV1. Each box plot represents the median, lower and upper quartiles (25th and 75th percentile) and whiskers represent the lower 10th and upper 90th percentile. Statistical significance was calculated by comparing ovarian cancer cell lines by Mann-Whitney test (**** $p<0.0001$).

4.1.1 Identification of a threshold of pH to discriminate CTC from WBC in clinical samples

To identify a threshold of extracellular acidification (i.e.: pH) able to better discriminate between hypermetabolic cells and WBC, the extracellular acidification of MDA-MB-231 and MCF7, which have a high and low metastatic potential, respectively, and WBCs were assessed by using the single-cell metabolic based assay. As shown in Figure 10A and B, both cancer cell lines had a significantly higher acidification rate respect to that detected in WBCs and, interestingly, MDA-MB-231 reached lower level of pH respect to MCF7, as previously described [147].

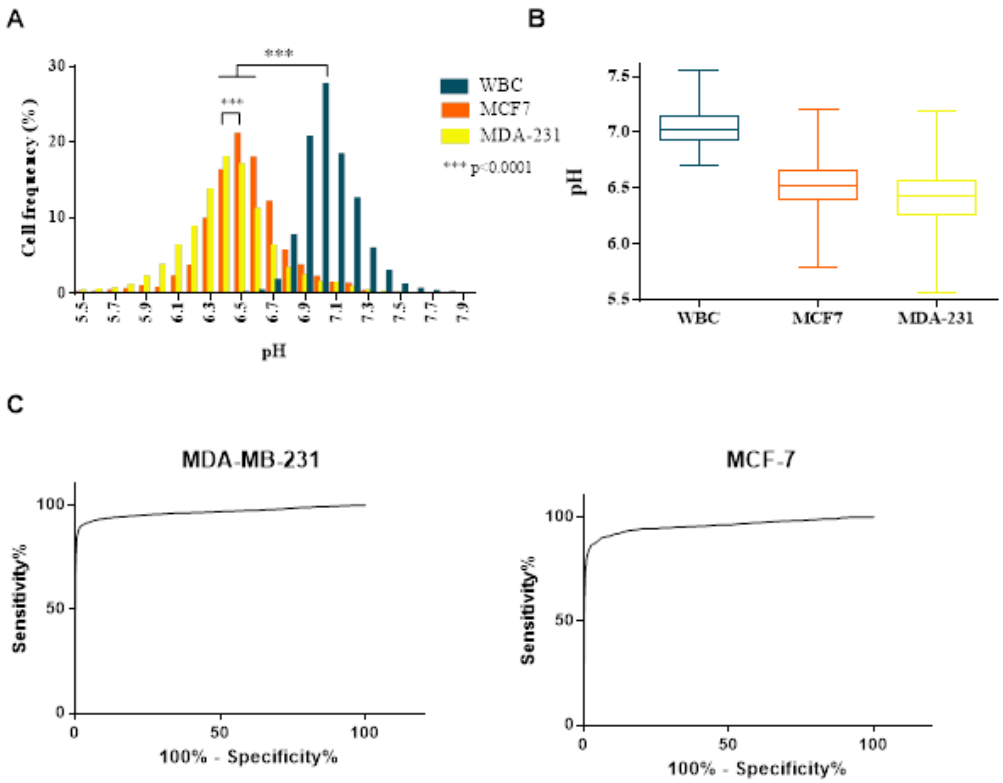

Figure 10. Measurement of extracellular acidification. A) Representative histogram reporting the acidification of cell-containing droplets for both breast cancer cell lines (MDA-MB-231 and MCF7) and WBCs obtained from healthy donor's sample. B) Comparison of extracellular acidification between breast cancer cell lines (MCF7 and MDA-MB-231) and WBCs. Each box plot represents the median, lower and upper quartiles (25th and 75th percentile) and whiskers represent the lower 10th and upper 90th percentile. Statistical significance was calculated comparing cell lines and WBCs by Mann-Whitney test. C) ROC curves obtained comparing the extracellular acidification of MDA-MB-231 and MCF7 breast cancer cell lines against WBC.

The threshold to distinguish hypermetabolic cells from WBC in patient's samples was set using ROC curve analysis of cancer cell lines (MDA-MB-231 and MCF7) and WBC (Figure 9C). The area under the curve revealed that the acidification measurement had an accuracy of 0.96 and 0.95 in discriminating MDA-MB-231 and MCF7, respectively, from WBC. A cut-off value of pH<6.4 were defined to ensure a specificity of 99.9% for both cancer cell lines; with the selected cut-off, the assay resulted in a sensitivity of 45% for the highly metastatic MDA-MB-231 and 22% for the low-metastatic MCF7.

Overall, the different behaviour of cancer cells and WBCs and the demonstrated ability of our method to report on the different explored conditions supported the previously described functional assay [147] to distinguish hypermetabolic cancer cells from WBCs by measuring their extracellular acidification. Thus, a clinical trial was designed to assess the potential of enumerating CTCs in blood samples from cancer patients.

4.2 Comparison of CTC detection rate with the metabolism-based and the CellSearch

4.2.1 Patient's characteristics

Between March and October 2017, 31 consecutive patients with MBC were recruited at the IRCCS-Centro di Riferimento Oncologico of Aviano, regardless of the number and type of previous treatment line(s). CTC enumeration was assessed before the beginning of a new line of treatment and after an average of 3.4±0.5 weeks following the first cycle of therapy. Patient demographics and tumour characteristics at the time of enrolment are summarized in Table 4.

The median age was 56. Primary tumour receptor status for ER and/or PR (detected by IHC) and HER2 overexpression (evaluated by IHC and FISH) were positive in 21 (68%) and 3 (10%) out of 31 patients, respectively, while 8 (26%) out of 31 cases were triple-negative (ER-, PR- and HER2-negative). Among the 31 patients recruited, 11 (35.5%) were starting their first line of therapy for metastatic disease, 28 (90%) received chemotherapy (alone or in combination with other treatments), 2 (6,5%) received hormone-therapy and 1 (3.2%) patient was in the control group of an experimental therapy and received placebo. Overall, at the end of the study disease progression was observed in 23 out of 31 cases, 6 out of them died. All patients had a minimal follow-up time of 9 month (median 15 months) for survival after the baseline collection of the blood sample. The results of the first imaging revaluation after the CTC enumeration documented a partial response in 13 patients out of

31 patients (42%). The average time between the baseline and the first follow-up imaging study among these 13 patients was 21±7.1 weeks.

	N	%
All patients	31	100.0
Age at baseline		
Median	56	
Range	39-78	
ER- and PR-receptor status		
ER+ or PR+	21	68.0
ER- and PR-	10	32.0
Her2/neu status		
Positive	3	10.0
Negative	28	90.0
Triple negative	8	26.0
Sites of metastasis		
Bone	23	74.0
Lung	14	45.0
Brain	2	6.0
Liver	14	45.0
Nodes	19	61.0
Number of metastasis		
1	9	29.0
2 or more	22	71.0
Therapy		
First line	11	35.5
Second line or subsequent	19	61.3
Not available	1	3.2
Type of therapy		
Chemotherapy	20	64.5
Chemotherapy and targeted therapy	8	25.8
Hormone-therapy	2	6.5
Palliative	1	3.2

Table 4. Patient and tumour characteristics.

4.2.2 Baseline CTC enumeration

The metabolism-based method was used to enumerate metabolically active CTCs in peripheral blood (PB) of 31 MBC patients and 26 healthy donor (HD) volunteers. Positive events were defined as droplet-containing cell with a pH below 6.4, negative for CD45 and positive or negative for EpCAM expression.

In the cohort of HDs, CTC-like events were detected only in 2 (7.6%) out of 26 HDs with an average of 0 ± 1 CTC/7.5 ml of blood (median 0, range 0-5) (Table 5).

ID		Metabolism-based assay	
		CTC	CTC E+
1	HD	0	0
2	HD	0	0
3	HD	0	0
4	HD	5	0
5	HD	0	0
6	HD	0	0
7	HD	0	0
8	HD	0	0
9	HD	0	0
10	HD	0	0
11	HD	0	0
12	HD	0	0
13	HD	0	0
14	HD	0	0
15	HD	4	4
16	HD	0	0
17	HD	0	0
18	HD	0	0
20	HD	0	0
21	HD	0	0
22	HD	0	0
23	HD	0	0
24	HD	0	0
25	HD	0	0
26	HD	0	0
	N	26	26
	Mean	0 ± 1	0 ± 1
	Median	0	0
	Range	0-5	0-4

Table 5. Prevalence of CTCs in the cohort of healthy donor (HD) volunteers. CTC = total circulating tumour cell; CTC E^+ = circulating tumour cells positive for EpCAM expression).

Thirty-one MBC enrolled in the study and 27 out of 31 were evaluable for baseline (T0) CTC count with the single-cell metabolism-based method, while 4 had to be excluded from prevalence analysis, since the baseline blood draw has been missed for organizational and/or technical failure (Figure 11). Overall, the numbers of CTCs were higher in PB samples of MBC patients than CTC-like cells in HD samples (p=0.001, Mann-Whitney U-test) (Figure 12). In more detail, 12 out of 27 patients (44.4%) had at least 1 detectable CTC/7.5 ml of PB; the average number of detected CTC was 218±1022 (median 0, range 0-5319). Among these CTC-positive patients, 6 cases (22.2%) presented a subpopulation

of CTCs defined as both acid- and EpCAM-positive with an average CTC count of 19 ± 53 in 7.5 ml of PB (median 0, range 0-200) (Table 6).

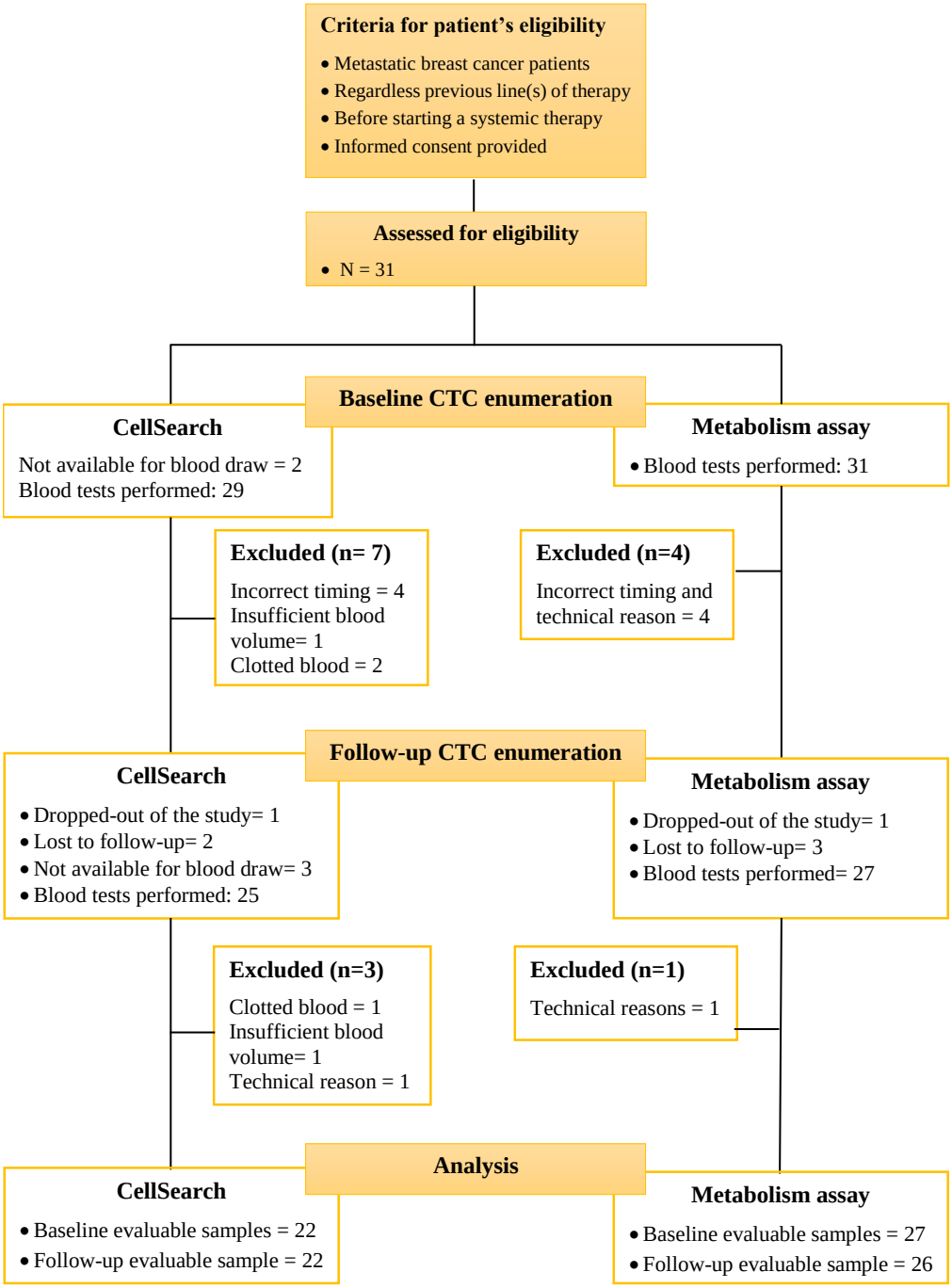

Figure 11. CONSORT diagram describing the study design, patient's enrolment and data exclusion reasons.

		Metabolism-based assay				CellSearch			
		T0		T1		T0		T1	
ID	Histology	CTC	CTC E+	CTC	CTC E+	CTC	CTC M30+	CTC	CTC M30+
1	ER+/PR+/HER2-	n.a.	n.a.	61	0	n.a.	n.a.	0	0
2	ER+/PR-/HER2-	n.a.	n.a.	121	0	n.a.	n.a.	0	0
3	ER+/PR+/HER2-	n.a.	n.a.	48	0	n.a.	n.a.	1	0
4	ER-/PR-/HER2-	n.a.	n.a.	n.a.	n.a.	n.a.	n.a.	0	0
5	ER-/PR-/HER2-	0	0	0	0	0	0	0	0
6	ER-/PR-/HER2-	375	200	280	160	379	25	127	7
7	ER-/PR-/HER2-	5319	194	243	18	2022	0	288	0
8	ER-/PR-/HER2-	14	14	0	0	21	0	0	0
9	ER-/PR-/HER2-	0	0	6	6	n.a.	n.a.	n.a.	n.a.
10	ER-/PR-/HER2-	55	0	n.a.	n.a.	0	0	n.a.	n.a.
11	ER+/PR-/HER2-	13	9	4	4	244	0	30	1
12	ER+/PR+/HER2-	6	0	n.a.	n.a.	n.a.	n.a.	-	-
13	ER+/PR-/HER2-	0	0	4	4	2	0	0	0
14	ER+/PR+/HER2-	0	0	38	22	31	0	0	0
15	ER-/PR-/HER2+	0	0	0	0	n.a.	n.a.	2	0
16	ER+/PR+/HER2-	22	17	5	0	1	0	1	0
17	ER+/PR-/HER2-	0	0	3	0	4	0	10	0
18	ER-/PR-/HER2-	0	0	0	0	1	1	-	-
19	ER+/PR+/HER2-	0	0	0	0	2	0	1	0
20	ER+/PR+/HER2-	0	0	133	122	0	0	0	0
21	ER-/PR-/HER2+	0	0	0	0	0	0	0	0
22	ER+/PR-/HER2-	67	67	4	0	3	0	-	-
23	ER+/PR+/HER2-	0	0	n.a.	n.a.	67	0	-	-
24	ER+/PR+/HER2-	0	0	3	0	2	0	0	0
25	ER+/PR+/HER2-	0	0	0	0	32	0	3	0
26	ER-/PR+/HER2-	3	0	0	0	n.a.	n.a.	n.a.	n.a.
27	ER+/PR+/HER2+	5	0	0	0	n.a.	n.a.	n.a.	n.a.
28	ER+/PR+/HER2-	6	0	4	0	16	0	0	0
29	ER+/PR-/HER2-	0	0	0	0	2	0	2	0
30	ER+/PR+/HER2-	9	0	0	0	4	1	10	0
31	ER+/PR+/HER2-	0	0	n.a.	n.a.	0	0	-	-
	N	27	27	26	26	22	22	22	22
	Mean ± S.D.	218±1022	19±53	37±75	13±38	129±433	1±5	22±65	0±1
	Median	0	0	4	0	3	0	1	0
	Range	0-5319	0-200	0-280	0-160	0-2022	0-25	0-288	0-7

Table 6. Prevalence of CTCs: comparison between the single-cell metabolism-based method and the CellSearch. The table reports patient data and CTC count of each patient at baseline (T0) and follow-up (T1), along with the corresponding prevalence of EpCAM positive (CTC E+) and apoptotic CTCs (CTC M30+) as detected with the metabolism-based method and CellSearch test, respectively. (n.a = not available data; see Figure 3 for details).

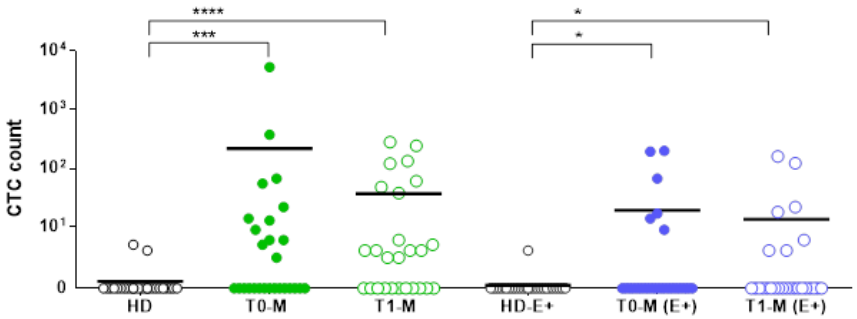

Figure 12. CTC count of healthy donor (HD) and MBC patients at baseline (T0) and follow-up (T1) performed with the metabolism-based assay (M). Overall, 26 healthy donors (HD) and 27 and 26 out of 31 enrolled patients were included for CTC enumeration at T0 and T1, respectively. The graph reports both the total CTC count (Acid-positive (pH<6.4) droplets containing CD45 negative and EpCAM-positive or negative cells and the prevalence of the subpopulation of EpCAM-positive (E+) CTCs. Horizontal bars represent the average CTC count. Statistical significance was evaluated by Mann-Whitney test (* p-value ≤ 0.05; *** p-value ≤ 0.001; **** p-value ≤ 0.0001).

Next, to assess the question whether the variation in the number of CTCs is also reflected in the clinical outcome, ROC curves were plotted to determine a cut-off level of CTCs to discriminate between MBC and HD (Figure 13); the area under the curve was 0.697 with 95% CI from 0.584 to 0.794 (p-value = 0.01377). Giving the nature of this pilot study and the comparative aim with the CellSearch, previously reported as a strong and independent predictor of survival with the threshold of ≥5 CTC [27,151], a cut-off value of ≥4 CTC was established to have 96% specificity with the metabolism-based method (Table 7). Stratifying the MBC patient's cohort for the threshold of ≥4 CTCs, 11 out 27 (40.7%) were categorized as CTC-positive.

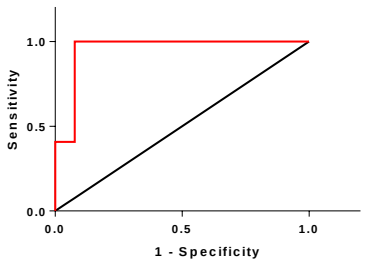

Area under the ROC curve	
Area	0,6973
Std. Error	0,0731
95% CI	0,5540 to 0,8406
p-value	0,01377

Figure 13. ROC curve for CTC count to discriminate patients from healthy donors and table summarizing the results of AUC analysis.

Cutoff	Sensitivity	95% CI	Specificity	95% CI
> 1.500	0,4444	0,2548 to 0,6467	0,9231	0,7487 to 0,9905
> 3.500	0,4074	0,2239 to 0,6120	0,9231	0,7487 to 0,9905
> 4.500	**0,4074**	**0,2239 to 0,6120**	**0,9615**	**0,8036 to 0,9990**
> 5.500	0,3704	0,1940 to 0,5763	1,0000	0,8677 to 1,000
> 7.500	0,2963	0,1375 to 0,5018	1,0000	0,8677 to 1,000
> 11.00	0,2593	0,1111 to 0,4629	1,0000	0,8677 to 1,000
> 13.50	0,2222	0,08622 to 0,4226	1,0000	0,8677 to 1,000
> 18.00	0,1852	0,06300 to 0,3808	1,0000	0,8677 to 1,000
> 38.50	0,1481	0,0419 to 0,3373	1,0000	0,8677 to 1,000
> 61.00	0,1111	0,0235 to 0,2916	1,0000	0,8677 to 1,000
> 221.0	0,0741	0,0091 to 0,2429	1,0000	0,8677 to 1,000
> 2847	0,0370	0,0009 to 0,1897	1,0000	0,8677 to 1,000

Table 7. Table summarizing the value of sensitivity and specificity calculated for each cut-off value along with their 95% confidence interval (CI) resulted from the comparison among HD and MBC patients. The cut-off with 96% specificity (highlighted in yellow) was chosen to discriminate between HD and MBC patients.

For a direct methods comparison, 29 out of 31 of the above described patients were available for CTC enumeration with the CellSearch platform. Thus, the same day that the blood draw for the single-cell based-method was retrieved, an additional sample for CellSearch analysis was collected. For the CellSearch method, data were not evaluable from 7 samples at T0, because of technical reasons such as insufficient blood volume or clotted blood (Figure 11). Overall, CTC count with CellSearch was available for 22 patients. In MBC the CellSearch assay identifies a high-risk patients group according to a cut-off value of $\geq$ 5 CTCs/7.5 ml PB [27,151]. When the cohort was stratified according to this criterion, 5 or more CTCs were found in 8 out of 22 (36%) patients (Table 6). As previously described, the M30 antibody, used in conjunction with the standard CellSearch kit, is a valuable tool to identify apoptotic CTC in MBC[152]. Since in this study we employed a method that aims to detect metabolically active and thus viable CTC, for comparative purpose, the M30 apoptosis marker was added to the CellSearch. Among the 17 patients which resulted positive for at least 1 CTC, 3 (17.6 %) were positive for the presence of at least one M30-positive CTC with an average CTC count of 1±5 (median 0, range 0-25). Instead, only 1 out of the 8 patients with a CTC number ≥5 CTC was positive with 25 M30-positive CTCs over a total of 379 CTCs (Table 6).

4.2.3 Follow-up CTC enumeration

At follow-up (T1), after a median of 3 weeks from the collection of the baseline time point, a total of 26 patients out of 31 were included in the analysis with the metabolism-based assay. Among the 31 recruited patients, 1 dropped-off the study, 3 were lost to follow-up, and 1 had to be excluded for technical reason (Figure 11).

Fifteen out of 26 patients (57,7%) presented at least 1 CTC in 7.5 ml of PB, while 13 out 26 (50%) were positive for the presence of 4 or more CTCs. In comparison to what observed at T0, the average number of CTCs decreased from 218±1022 to 37±75 (median 4, range 0-280) (Table 6 and Figure 12). Furthermore, the number of CTC-positive patients presenting an EpCAM positive subpopulation remained almost unchanged, accounting for 7 cases out of 26 (26,9%), with an average CTC count of 13±39 (median 0, range 0-160) (Table 6 and Figure 12).

From the comparison of the CTC levels between T0 and T1, the CTC level fell in 10 cases and increased in 6, while 7 patients remained CTC-negative before and after chemotherapy (0 at both T0 and T1). The CTC enumeration between T0 and T1 was not statistically different (p=0.2465, Wilcoxon test).

For the parallel CellSearch analysis, 25 out 31 recruited patients were available for CTC enumeration with the CellSearch test. Three samples had to be excluded from analysis since the patients dropped-out of the study or because of technical reasons such as insufficient blood volume or clotted blood samples (Figure 11). Overall, CTC count with CellSearch was available for 22 patients at T1.

When considering the cut-off value of ≥5 CTC/7.5ml of PB, the number of CTC positive patients decreased to 5 out 22 (23%) and the average CTC number decreased from 129±433 to 22±66 (median 1, range 0-288) compared to what detected at T0 (Table 6).

Patients presenting apoptotic CTCs were detectable also at T1. In more detail, 2 (9,1%) out of 22 samples were positive for the presence of at least one $M30^+$ positive CTC, with an average count that decreased to 0±1 CTC (median 0, range 0-7), respect to that at T0.

In this cohort, 17 patients had matched blood samples between T0 and T1 and 2 (11,8%) cases had an increase and 10 (58,8%) a decrease in CTC levels, while there were 5 (29,4%) cases with unchanged CTC numbers. The CTC enumeration between T0 and T1 was statistically different (p=0.0146, Wilcoxon test) (Figure 14).

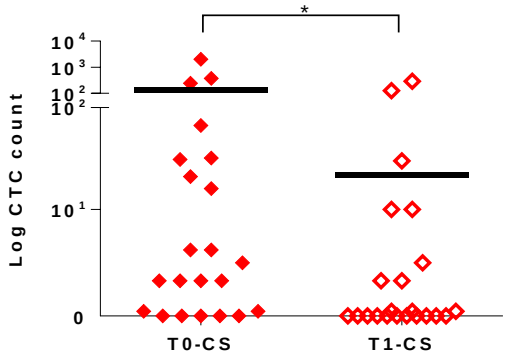

Figure 14. CTC enumeration of MBC patients at baseline (T0) and follow-up (T1) performed with the CellSearch (CS). Overall, 22 out of 31 enrolled patients were evaluable for CTC enumeration at T0 and T1, respectively. Horizontal bars represent the mean average CTC count. Statistical significance was evaluated by Wilcoxon test (* p-value ≤ 0.05).

4.2.4 Comparison of CTC levels obtained by using the metabolic based assay and CellSearch

Among all recruited patients (n=31), a total of 22 and 21 cases had matched blood samples between the metabolism-based method and the CellSearch analysis at both T0 and T1.

As shown in Figure 15A and B, the average CTC count was higher when evaluated with the metabolism-based assay compared to the CellSearch system at both time points. However, the CTC enumeration between the two methods was not statistically different both at T0 (Wilcoxon test, p=0.410) and T1 (Wilcoxon test, p=0.175). Moreover, the direct comparison of matched blood samples revealed weak or absence of correlation among paired samples at T0 and T1, respectively (T0: Spearman r =0.39; T1: Spearman r = 0.04) (Figure 14 C e D).

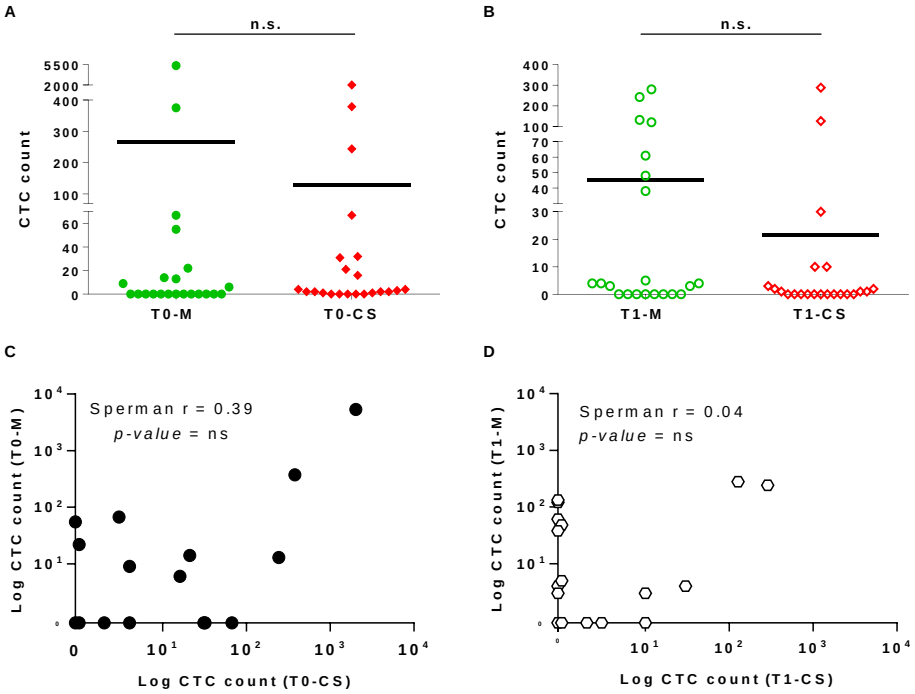

Figure 15. Direct method comparison of CTC enumeration with the metabolism-based method (M) and the CellSearch (CS) system at baseline (T0) (A and C) and follow-up (T1) (B and D). Only complete data sets that include results from both the metabolism-based method and the CellSearch were plotted. Overall, 22 and 21 cases had matched blood sample at T0 and T1, respectively. Statistical significance was evaluated by Wilcoxon test.

Using the cut-off values of ≥5 and ≥4 CTCs for the CellSearch and the metabolism-based assay, respectively, the overall positive concordance was 68.2%, at T0, and 52.4% at T1. Applying these cut-offs, the number of patients scoring negative for the CellSearch assay while positive for the metabolism-based method were 4 out of 14 (28.6%), at T0, and 8 out 16 (50%), at follow-up.

Finally, as demonstrated by the low k-Cohen coefficient (Table 8), comparison between the two methods revealed to be low.

Method	CellSearch		
Metabolism-method	**<5**	**≥5**	**Tot**
T0 [a]			
<4	10	3	*13*
≥4	4	5	*9*
Tot	*14*	*8*	*22*
T1 [b]			
<4	8	2	*10*
≥4	8	3	*11*
Tot	*16*	*5*	*21*

a Kappa = 0.330 (fair agreement); SE of kappa = 0.205; 95% CI from -0.071 to 0.732; Number of observed agreements: 15 (68.2% of the observations);
b Kappa = 0.180 (poor agreement); SE of kappa = 0.218; 95% CI from -0.282 to 0.423; Number of observed agreements: 11 (52.4 % of the observations).

Table 8. Concordance of CTC status between CellSearch and metabolism-based assay at baseline (T0) and follow-up (T1). To define a patient as CTC-positive, the threshold of ≥5 and ≥4 CTCs/7.5 ml of PB was used for CellSearch and metabolism-based assay, respectively.

As shown in Table 6, comparing patients who presented apoptotic CTCs at T0 with the CellSearch, 2 out of 3 patients had a positive CTC count with the metabolism-based assay, while the other one was negative. Interestingly, among the 19 patients defined as negative for apoptotic CTCs by CellSearch, 7 (36%) were instead positive for the presence of CTCs with both methods. At T1, 2 out of 2 patients positive for the presence of apoptotic CTC were also positive for the metabolism-based assay, while among the 19 patients negative for M30 marker, 8 (42%) were positive for the metabolism-based assay and 4 out of these patients were scored positive also by the CellSearch for the presence of CTCs. Overall, these results suggested that the presence of apoptotic cells in this cohort of patients was low.

4.2.4 Survival analysis of the metabolism-based method and the CellSearch system

To evaluate the presence of CTCs as a predictor of overall (OS) and progression free (PFS) survival, patients were stratified into those with ≥4 CTCs, for the metabolism-based method, and with ≥5 CTCs for the CellSearch. In Figure 16 and 17, Kaplan-Meier curves for the different CTC cut-off values at both T0 and T1 time points are shown.

Among the 31 patients enrolled, the presence of 4 or more CTCs showed to be associated with a worse OS with the metabolism-based method (p=0.0030 and p=0.0059), and similar

results were obtained by stratifying the patient's cohort by the cut-off value of ≥5 CTC with the CellSearch system (p= 0.0148 at T0, p= 0.0245 at T1) (Figure 16).

CTC-positive patients showed a significant shorter median PFS respect to CTC-negative patients (127 days vs 287; p=0.0017) at T0, and, as well, at T1 (140 vs 360 days, p= 0.0065) (Figure 17), as assessed by the metabolism-based method.

For the CellSearch analysis, patients with an unfavourable number of CTC (≥5 CTC/7.5 ml of PB) had a significantly shorter median PFS both at T0 (131 and 262 days, p=0.0206) and at T1 (119 days vs 264 days, p= 0.00346).

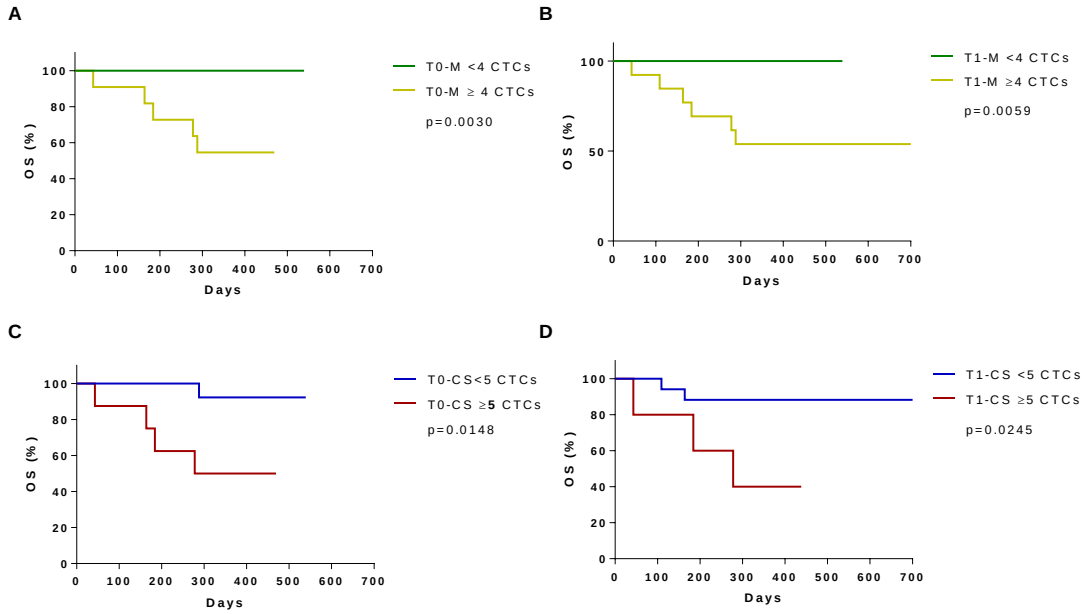

Figure 16. Kaplan-Meier plot estimating OS of MBC at T0 (A and C) and at T1 (B and D) by single-cell-metabolism assay (M) and for the CellSearch test (B and D). For this analysis, patients were stratified using a cut-off value of <4 or ≥ 4 CTCs (A and B) or <5 or ≥5 CTCs (C and D) for the metabolism-based (M) and CellSearch (CS) method, respectively.

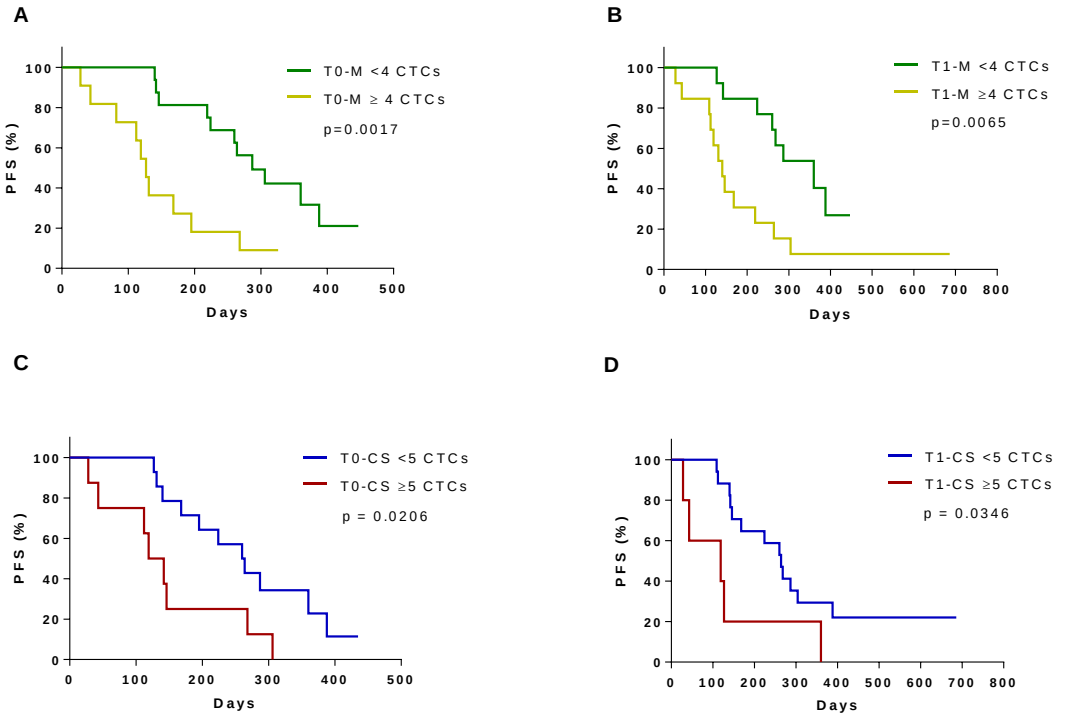

Figure 17. Kaplan-Meier plot estimating PFS of MBC at T0 (A and C) and at T1 (B and D) by single-cell-metabolism assay (M) and CellSearch (C). For this analysis, patients were stratified using a cut-off value of <4 or ≥ 4 CTCs for the metabolism-based assay methods and <5 or ≥ 5 CTCs for the CellSearch.

4.3 Mutational analysis of CTCs positive using the metabolism-based method

In order to give a proof-of-concept that CTCs are present in the group of cells with high extracellular acidification level, a sorting device previously described by *Mazutis et al*. was employed [145]. This device allows to harvest the content of desired droplets by a dielectrophoretic pulse. First, capture efficiency of fluorescently labelled cells was evaluated. Thus, 50000 pre-stained cells were emulsified, and 1000 cell-containing droplets were sorted out. The average recovery efficiency was 77±16%.

Then, 5 MBC hormone refractory patients were analysed. Droplets containing cells that exhibited a pH below 6.4 were sorted out of the device. The presence of the most common hotspot mutations in ESR1 (Y537N, D538G, L536R) was assessed by ddPCR. From the analysis of DNA obtained from hypermetabolic cells, ESR1 was found mutated in 3 out 5 patients. In particular, one patient showed the presence for both Y537N and L536R mutations, one was positive for the Y537N and D538G hotspots and the last presented mutant DNA copies only for the hotspot Y537N (Figure 18). The other two patients were

found positive for PI3KCA E545K and H1047R, thus confirming that CTCs were present in the harvested pool of cells.

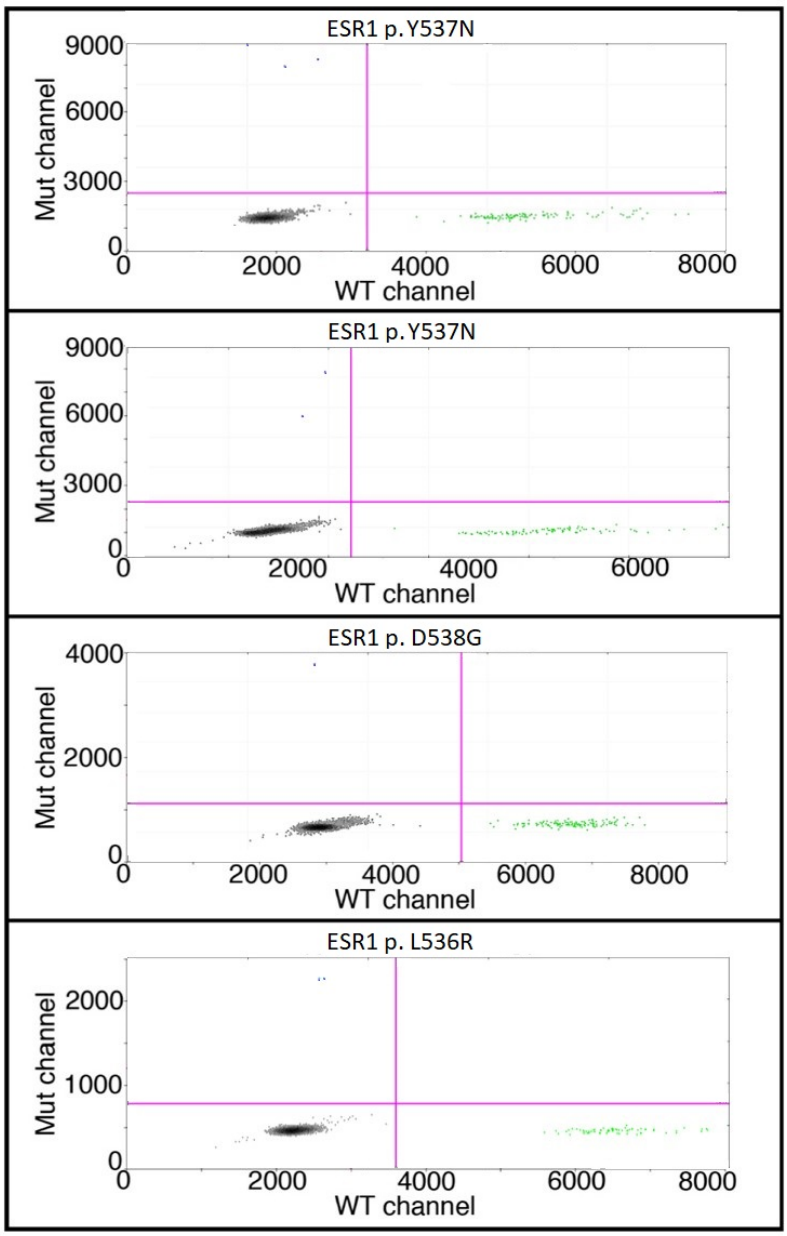

Figure 18. 2-dimensional dot-plots showing the results of ddPCR of four representative patients in which mutated DNA was detected. In Y-axis: intensity of FAM dye tagging mutated DNA (Mut channel); in X-axis: intensity of HEX dye tagging wild type DNA (WT channel). Grey droplets are empty, green droplets contain wild type DNA, and blue droplets contain mutated DNA.

5. DISCUSSION

Despite the great advances in the early diagnosis and treatment, BCs ranks among the leading cause of cancer-related death in women worldwide and its metastatic spread still represents the main cause of cancer-related death. Thus, there is a clear clinical need of effective biomarkers able to detect cancer at early stage, stratify the patient population which most likely will benefit from a specific therapy, monitor the treatment response, quantify the minimal residual disease and assess the emergence of therapy resistance[13].

CTCs are considered as a surrogate of cancer in blood and have gained attention as one of the most promising approaches to face the aforesaid needs in the clinical management of cancer as detection of CTCs is a non-invasive tool that could provide real-time information on the evolving biology of both primary tumour and metastatic sites [14,93,153–155].

The only currently FDA-approved technology for CTCs in MBC is the CellSearch® platform that typically processes fixed blood samples and detect CTC relying on the expression of EpCAM on their surface. This technology has widely demonstrated the prognostic and predictive value of evaluating the number [10,29,83,156], and/or variation in the level, [10,28,157] of CTCs in patients with early and metastatic BC. However, CTCs has failed to reach the clinical routine because of a lack of demonstration of their clinical utility.

The common use of EpCAM to enrich CTCs from blood is considered one of the major limitations of the CellSearch® and other EpCAM-based technology, as EpCAM might be downregulated by CTCs due to the EMT process, thus leading to an underestimation of CTCs [51]. Several studies have indeed demonstrated the presence of EpCAM-negative CTC in blood from cancer patients of several types, including MBC, and their association with a worst prognosis [46,77]. Thus, waiting for the results of other ongoing interventional trial based on CTC enumeration to guide therapy decision (e.g.: French CirCé01 trial and STIC CTC trials)[83], it is not surprisingly that the field of CTC research has switched to the characterization of CTC by testing other technologies, which exploit other cancer features, with the hope to find more of these rare cancer cells and, obviously, the highly desired clinical benefit [51].

Reprogramming of metabolism is a recognized hallmark of cancer and it is commonly associated to an increased glucose uptake and consumption. As a direct consequence of metabolic alterations, many cancers exhibit abnormal lactate release coupled with a proton H^+, which leads to the acidification of the tumour microenvironment. Indeed, it is well established that tumour tissue has an acidic pH which has a recognized role in cancer

invasion and metastasis [158]. Interestingly, this phenomenon occurs early in carcinogenesis, and it is important for cancer cells to gain selective advantages and a more metastatic phenotype [158]. Even if such metabolic alterations are well-known, to best of our knowledge, they have never been used to detect CTCs.

To address the question whether putative CTCs with an altered metabolism can be detected in blood sample of cancer patients, our group developed a single-cell metabolism-based assay based on the differential extracellular acidification level between normal and cancer cells. This assay exploits a droplet microfluidic technology, which allows to compartmentalize single-cell into a droplet and detect hypermetabolic cells by pH measurements of the extracellular space [147]. To avoid a lack of resolution and bias on the resulting detected pH, we used an unbuffered cell culture medium, to allow an accurate measurement of proton release, and a ratiometric pH-sensitive dye (SNARF-5F) for pH readout.

Our droplet-based microfluidic approach is typically used for the encapsulation of cells, as it allows to maintain cell growth and proliferation properties, and the screen for secreted molecules, as they are retained inside the droplet [144,145,159,160]. Using cancer cell lines with different metastatic potential and normal blood cells, we demonstrated that the differential proton release rate can be detected in-drop exploiting a pH-sensitive dye. This is supported by several observations.

The system was able to discriminate among different population of acidic droplets and we were able to measure variation in the extracellular acidification both in time and under the stimulation of increasing concentration of glucose, which typically boost the acidification rate of cancer cells. Moreover, comparing two breast cancer cell lines, MDA-MB-231 and MCF7, we found that the highly metastatic MDA-MB-231 reached lower pH values compared to the low metastatic MCF7, and that both had a higher acidification rate compared to WBC. Similarly, we found consistency between the previously described metabolic feature of OC316 and IGROV-1 ovarian cancer cells lines. Indeed, the pH measurements, as detected with our system, showed concordant result with that reported with the proton flux analyzer SeahorseFX, finding that the high glycolytic OC316 had a higher rate of acidification respect to the low glycolytic IGROV-1[150]. Finally, as the pH correspond to the concentration of proton H^+ and, thus, depends from the volume on which such measurement is performed, when testing the pH of cancer cells encapsulated in droplet of increasing size, we could observe, as expected, that cells reach less acidic pH values.

With the aim of applying this metabolism-based method in a clinical setting, we first investigated on several technical issues to have a firmly established method to process blood sample from cancer patients. First, we investigated on the effect of room temperature, finding that a temperature control system is mandatory to inhibit the release of proton over the time of analysis of clinical samples, which could otherwise introduce biases on single-cell pH measurements. Secondly, we set up the best condition for encapsulating single-cell. We have chosen a volume droplet size which allowed us to discriminate cancer cells from WBC after a time of incubation considered reasonable for future application in a diagnostic setting.

Finally, using the breast cancer cell lines MDA-MB-231 and MCF7, we established a functional cut-off value, i.e.: the pH value, for discriminating CTC from WBC in clinical sample. Given the exploratory nature of this study, we choose a cut-off value of pH<6.4, which favors specificity respect to sensitivity as detected from the ROC curves plotted between breast cancer cell lines and WBC. Using this functional cut-off of pH, the single-cell metabolism-based method showed that up to 45% and 22% of MDA-MB-231 and MCF7, respectively, could be detected. This partial selection may have been due to the heterogeneity of the cancer cell line population, a feature widely reported in literature, and that could not be appreciated from bulk measurement as those performed from system like the SeahorseFX. This suggest that our microfluidic platform can represent an alternative for the direct measurement of proton release at single cell level, giving the possibility to distinguish heterogeneous acidifying CTCs. However, these sensitivities are in line with that obtained by other works reporting data using viable cells in spike-in experiments and it cannot be excluded that at least a part of the cell is not able to reach higher pH value because of the death program induced by anoikis or because of handling procedure. Finally, using this cut-off value of pH to discriminate between normal blood cells and CTCs, among 26 HD volunteers we found only a negligible background of positive events (range 0-5) and only in 2 (7.6%) out of 26 HD.

Despite many of the promising technologies introduced over the last decade demonstrated a higher rate of CTCs detection respect to CellSearch, often they do not address the question whether the identified subpopulation of CTCs has a clinical relevance [51]. Further, lacking for a solid system able to really quantify the concentration of CTC, at least the difference between the identified CTC and those detected with the CellSearch® system should be provided but, instead, is often missing [51]. Thus, having the method firmly established, we designed a pilot clinical study to investigate on the potential of enumerating CTCs in blood

samples from MBCs and we compared our method to the CellSearch®, as it represents the gold standard system for CTC count in the peripheral blood of MBC patients [10].

In this study, the presence of CTCs as detected by the metabolism-based method in a cohort of 31 MBC patients resulted to be significantly higher than that observed in the HD volunteers and moreover it showed a broad range in the number of detected CTCs (range 0-5319 at T0 and 0-280 at T1). The number of CTCs identified by our method was on average higher than that obtained with the CellSearch both at T0 and T1 although this difference was not statistically significant. Thus, it should be validated in a larger cohort of patients.

Our data indicated a low agreement among the two methods, that was more evident at the follow-up time point. These results suggest that the two techniques could detect partially overlapping different populations of CTCs that can be complementary in predicting the progression of the disease. Interestingly, we observed that our system was a predictor of both OS and PFS compared to that observed with the CellSearch system.

From the analysis performed with CellSearch regarding the expression of M30 as an apoptotic marker, we could observe a low presence of apoptotic CTCs, suggesting that CTCs detected in this cohort of MBC are mainly viable, at least in regard to EpCAM- and CK-positive cells. As previously demonstrated, non-apoptotic CTCs have a highly metastatic potential and the fact that there was a correspondence between the patient negative for the expression of M30 and the presence of metabolically active CTCs, lead us to speculate that CTCs as detected by our method are indeed viable CTC.

Recently, interesting findings have been reported in support of the hypothesis that metabolic alterations, in particular the elevated glucose uptake, is a feasible tool to identify hypermetabolic CTCs in the PB of metastatic cancer patients [161–165]. For instance, *Tang et al* evaluated the presence of metabolically active tumour cells in pleural effusion and in a limited number of PB of NSCLC by using 2-NBDG and confirmed their neoplastic nature via single-cell sequencing. These evidences were recently strengthened by our group in a separate study, which assessed the mutational status of hypermetabolic CTCs enriched for their elevated 2-NBDG uptake and sorted by FACS. In more details, 30 metastatic NSCLC patients were screened for the presence of hypermetabolic CTCs and the mutational analysis of sorted cells were assessed for EGFR and KRAS mutations, showing both a positive concordance and the detection of new mutations in comparison with the primary tumour analysis[162]. Another recent study reports that, using a multiple RNA in situ hybridization technique, CTC positive for glucose metabolic genes were detectable in 35

out of 54 prostate cancer patients and the increase of this population of this glucose positive CTC was associated with advanced tumour stage and metastasis, performing better as a biomarker of metastasis compared to EMT marker. Other microfluidic platform have been described for the screening of single cell uptake of glucose, or exploiting the release of by-product of metabolism such as lactate[160] or ROS[166]. However, these studies report data mainly on cancer cell line or on a limited number of blood samples from cancer patients.

Further, we used ddPCR to confirm that the sorted fraction contained cells originating from the tumour and we observed the presence of characteristic hotspot resistance point mutations in ESR1 and PI3KCA, as previously reported in MBC patients [75]. This suggested that CTCs are indeed present in the group of hypermetabolic cells and further molecular analysis are ongoing to better characterize other samples. An interesting perspective would be to screen the mutational status of other genes implicated in the reprogramming of metabolism at the single cell level, along with a characterization of the expression of glycolytic enzyme typically deregulated in cancer.

In conclusion, in this work we successful implemented the analytical procedures of a prototype device that permitted to quantify CTCs based on their deregulated metabolism. This is an innovative functional method, because the comparison with the golden standard for CTC enumeration suggested that our device recognize partially overlapping population of CTCs.

Furthermore, the pilot study conducted in a cohort of 31 MBC patients demonstrated the association of the number of metabolically active cells with patients' outcome, strongly supporting the clinical validity of our device and offers a strong rationale to design a broader clinical study, especially devoted to confirm and validate these data, with particular regard to establish a cut-off value of worst prognosis for high burden of hypermetabolic cells.

Between the several therapeutic strategies, the reprogramming of tumour metabolism is one of the most promising and in this perspective, we think that our test might be used in the future to follow-up patients undergoing these therapies.

6. REFERENCES

1. Hanahan D, Weinberg RA. Hallmarks of cancer: The next generation. *Cell*. 2011;144(5):646-674.
2. Vogelstein B, Papadopoulos N, Velculescu VE, et al. Cancer Genome Landscapes. *Science (80-)*. 2013;339(6127):1546-1558. doi:10.1126/science.1235122.
3. Hanahan D, Weinberg RA. Hallmarks of cancer: The next generation. *Cell*. 2011;144(5):646-674. doi:10.1016/j.cell.2011.02.013.
4. Heymach J, Krilov L, Alberg A, et al. Clinical cancer advances 2018: Annual report on progress against cancer from the American Society of Clinical Oncology. *J Clin Oncol*. 2018;36(10):1020-1044. doi:10.1200/JCO.2017.77.0446.
5. Ferlay J, Soerjomataram I, Dikshit R, et al. Cancer incidence and mortality worldwide: Sources, methods and major patterns in GLOBOCAN 2012. *Int J Cancer*. 2015;136(5):E359-E386. doi:10.1002/ijc.29210.
6. Crowley E, Di Nicolantonio F, Loupakis F, Bardelli A. Liquid biopsy: Monitoring cancer-genetics in the blood. *Nat Rev Clin Oncol*. 2013;10(8):472-484. doi:10.1038/nrclinonc.2013.110.
7. Burrell RA, McGranahan N, Bartek J, Swanton C. The causes and consequences of genetic heterogeneity in cancer evolution. *Nature*. 2013;501(7467):338-345. doi:10.1038/nature12625.
8. Collisson EA, Campbell JD, Brooks AN, et al. Comprehensive molecular profiling of lung adenocarcinoma. *Nature*. 2014;511(7511):543-550. doi:10.1038/nature13385.
9. Duffy MJ. Serum tumor markers in breast cancer: Are they of clinical value? *Clin Chem*. 2006;52(3):345-351. doi:10.1373/clinchem.2005.059832.
10. Cristofanilli M, Budd T, Ellis M, et al. Circulating Tumor Cells, Disease Progression, and Survival in Metastatic Breast Cancer. *N Engl J Med*. 2004;351(8):781-791. doi:10.1056/NEJMoa040766.
11. Alunni-Fabbroni M, Müller V, Fehm T, Janni W, Rack B. Monitoring in metastatic breast cancer: Is imaging outdated in the era of circulating tumor cells? *Breast Care*. 2014;9(1):16-21. doi:10.1159/000360438.
12. Fazel R. Exposure to Low-Dose Ionizing Radiation from Medical Imaging Procedures Reza. *N Engl J Med*. 2010;363(1):1-3. doi:10.1056/NEJMp1002530.
13. Siravegna G, Marsoni S, Siena S, Bardelli A. Integrating liquid biopsies into the

management of cancer. *Nat Rev Clin Oncol*. 2017;14(9):531-548. doi:10.1038/nrclinonc.2017.14.

14. Alix-Panabières C, Pantel K. Clinical applications of circulating tumor cells and circulating tumor DNA as liquid biopsy. *Cancer Discov*. 2016;6(5):479-491. doi:10.1158/2159-8290.CD-15-1483.
15. Alix-Panabières C. Challenges in circulating tumour cell research. *Nat Rev Cancer*. 2014;14(3):152. doi:10.1038/nrc3686.
16. Micalizzi DS, Maheswaran S, Haber DA. A conduit to metastasis : circulating tumor cell biology. 2017:1827-1840. doi:10.1101/gad.305805.117.sion.
17. Krebs MG, Metcalf RL, Carter L, Brady G, Blackhall FH, Dive C. Molecular analysis of circulating tumour cells - Biology and biomarkers. *Nat Rev Clin Oncol*. 2014;11(3):129-144. doi:10.1038/nrclinonc.2013.253.
18. Alix-panabières C, Mader S, Pantel K. Epithelial-mesenchymal plasticity in circulating tumor cells. *J Mol Med*. 2016;95(2):133-142. doi:10.1007/s00109-016-1500-6.
19. Nieto MA, Huang RYYJ, Jackson RAA, Thiery JPP. Emt: 2016. *Cell*. 2016;166(1):21-45. doi:10.1016/j.cell.2016.06.028.
20. Aceto N, Bardia A, Miyamoto DT, et al. Circulating tumor cell clusters are oligoclonal precursors of breast cancer metastasis. *Cell*. 2014;158(5):1110-1122. doi:10.1016/j.cell.2014.07.013.
21. Hou JM, Krebs MG, Lancashire L, et al. Clinical significance and molecular characteristics of circulating tumor cells and circulating tumor microemboli in patients with small-cell lung cancer. *J Clin Oncol*. 2012;30(5):525-532. doi:10.1200/JCO.2010.33.3716.
22. Bethel K, Kuhn P. Circulating Tumor Cells : Fluid Surrogates of Solid Tumors. 2017. doi:10.1146/annurev-pathol-052016-100256.
23. Ashworth T. A case of cancer in which cells similar to those in the tumours were seen in the blood after death. *Aust Med J*. 1869. doi:10.1111/j.1528-1167.2011.03138.x.
24. Salgado I, Hopkirk JF, Long RC, Ritchie AC, Ritchie S, WEBSTER DR. Tumour cells in the blood. *Can Med Assoc J*. 1959;81(8):619-622.
25. Alexander RF, Spriggs AI. The differential diagnosis of tumour cells in circulating blood. *J Clin Pathol*. 1960;13:414-424. doi:10.1136/jcp.13.5.414.
26. Racila E, Euhus D, Weiss a J, et al. Detection and characterization of carcinoma

cells in the blood. *Proc Natl Acad Sci U S A*. 1998;95(April):4589-4594. doi:10.1073/pnas.95.8.4589.

27. Cristofanilli M, Budd G. Circulating tumor cells, disease progression, and survival in metastatic breast cancer. *Engl J Med*. 2004;351(8):781-791. doi:10.1056/NEJMoa040766.
28. Hayes DF, Cristofanilli M, Budd GT, et al. Circulating tumor cells at each follow-up time point during therapy of metastatic breast cancer patients predict progression-free and overall survival. *Clin Cancer Res*. 2006;12(14 Pt 1):4218-4224. doi:10.1158/1078-0432.CCR-05-2821.
29. Riethdorf S, Fritsche H, Mu V, et al. Detection of Circulating T umor Cells in Peripheral Blood of Patients with Metastatic Breast Cancer : A Validation Study of the CellSearch System. 2007;13(3):920-929. doi:10.1158/1078-0432.CCR-06-1695.
30. Deng G, Krishnakumar S, Powell AA, et al. Single cell mutational analysis of PIK3CA in circulating tumor cells and metastases in breast cancer reveals heterogeneity, discordance, and mutation persistence in cultured disseminated tumor cells from bone marrow. *BMC Cancer*. 2014;14(1). doi:10.1186/1471-2407-14-456.
31. Talasaz AH, Powell AA, Huber DE, et al. Isolating highly enriched populations of circulating epithelial cells and other rare cells from blood using a magnetic sweeper device. *Proc Natl Acad Sci*. 2009;106(10):3970-3975. doi:10.1073/pnas.0813188106.
32. Powell AA, Talasaz AAH, Zhang H, et al. Single cell profiling of Circulating tumor cells: Transcriptional heterogeneity and diversity from breast cancer cell lines. *PLoS One*. 2012;7(5). doi:10.1371/journal.pone.0033788.
33. Jan YJ, Chen JF, Zhu Y, et al. NanoVelcro rare-cell assays for detection and characterization of circulating tumor cells. *Adv Drug Deliv Rev*. 2018;125:78-93. doi:10.1016/j.addr.2018.03.006.
34. Gorges TM, Penkalla N, Schalk T, et al. Enumeration and Molecular Characterization of Tumor Cells in Lung Cancer Patients Using a Novel In Vivo Device for Capturing Circulating Tumor Cells. *Clin Cancer Res*. 2016;22(9):2197-2206. doi:10.1158/1078-0432.CCR-15-1416.
35. Kuske A, Gorges TM, Tennstedt P, et al. Improved detection of circulating tumor cells in non-metastatic high-risk prostate cancer patients. *Sci Rep*. 2016;6(1):39736. doi:10.1038/srep39736.

36. Andreopoulou E, Yang LY, Rangel KM, et al. Comparison of assay methods for detection of circulating tumor cells in metastatic breast cancer: AdnaGen AdnaTest BreastCancer Select/Detect™ versus Veridex CellSearch™ system. *Int J Cancer*. 2012;130(7):1590-1597. doi:10.1002/ijc.26111.
37. Müller V, Riethdorf S, Rack B, et al. Prognostic impact of circulating tumor cells assessed with the CellSearch System™ and AdnaTest Breast™ in metastatic breast cancer patients: the DETECT study. *Breast Cancer Res*. 2012;14(4):1-8. doi:10.1186/bcr3243.
38. Miltenyi S, Müller W, Weichel W, Radbruch A. High gradient magnetic cell separation with MACS. *Cytometry*. 1990;11(2):231-238. doi:10.1002/cyto.990110203.
39. Liu Z, Fusi A, Klopocki E, et al. Negative enrichment by immunomagnetic nanobeads for unbiased characterization of circulating tumor cells from peripheral blood of cancer patients. *J Transl Med*. 2011;9:70. doi:10.1186/1479-5876-9-70.
40. He W, Kularatne SA, Kalli KR, et al. Quantitation of circulating tumor cells in blood samples from ovarian and prostate cancer patients using tumor-specific fluorescent ligands. *Int J Cancer*. 2008;123(8):1968-1973. doi:10.1002/ijc.23717.
41. de Wit S, van Dalum G, Lenferink ATM, et al. The detection of EpCAM+ and EpCAM– circulating tumor cells. *Sci Rep*. 2015;5:12270. doi:10.1038/srep12270.
42. Vona G, Sabile A, Louha M, et al. Isolation by Size of Epithelial Tumor Cells. 2000;156(1):57-63. doi:10.1016/S0002-9440(10)64706-2.
43. Rosenberg R, Gertler R, Friederichs J, et al. Comparison of Two Density Gradient Centrifugation Systems for the Enrichment of Disseminated Tumor Cells in Blood. 2002;158:150-158. doi:10.1002/cyto.10161.
44. Gupta V, Jafferji I, Garza M, et al. ApoStream™, a new dielectrophoretic device for antibody independent isolation and recovery of viable cancer cells from blood. *Biomicrofluidics*. 2012;6(2):024133. doi:10.1063/1.4731647.
45. Fabbri F, Carloni S, Zoli W, et al. Detection and recovery of circulating colon cancer cells using a dielectrophoresis-based device : KRAS mutation status in pure CTCs. *Cancer Lett*. 2013;335(1):225-231. doi:10.1016/j.canlet.2013.02.015.
46. Bulfoni M, Gerratana L, Del Ben F, et al. In patients with metastatic breast cancer the identification of circulating tumor cells in epithelial-to-mesenchymal transition is associated with a poor prognosis. *Breast Cancer Res*. 2016;18(1):30. doi:10.1186/s13058-016-0687-3.

47. Nagrath S, Sequist L V, Maheswaran S, et al. Isolation of rare circulating tumour cells in cancer patients by microchip technology. *Nature*. 2007;450(7173):1235-1239. doi:10.1038/nature06385.
48. Sollier E, Go DE, Che J, et al. Size-selective collection of circulating tumor cells using Vortex technology. *Lab Chip*. 2014;14(1):63-77. doi:10.1039/c3lc50689d.
49. Dhar M, Wong J, Karimi A, et al. High efficiency vortex trapping of circulating tumor cells. *Biomicrofluidics*. 2015;9(6). doi:10.1063/1.4937895.
50. Che J, Yu V, Dhar M, et al. Classification of large circulating tumor cells isolated with ultra-high throughput microfluidic Vortex technology. *Oncotarget*. 2016;7(11):12748-12760. doi:10.18632/oncotarget.7220.
51. Parkinson DR, Dracopoli N, Gumbs Petty B, et al. Considerations in the development of circulating tumor cell technology for clinical use. *J Transl Med*. 2012;10(1):138. doi:1479-5876-10-138 [pii]\r10.1186/1479-5876-10-138.
52. Miller MC, Doyle G V., Terstappen LWMM. Significance of Circulating Tumor Cells Detected by the CellSearch System in Patients with Metastatic Breast Colorectal and Prostate Cancer. *J Oncol*. 2010;2010:1-8. doi:10.1155/2010/617421.
53. Coumans FAW, Ligthart ST, Uhr JW, Terstappen LWMM. Challenges in the enumeration and phenotyping of CTC. *Clin Cancer Res*. 2012;18(20):5711-5718. doi:10.1158/1078-0432.CCR-12-1585.
54. Ferreira MM, Ramani VC, Jeffrey SS. Circulating tumor cell technologies. *Mol Oncol*. 2016;10(3):374-394. doi:10.1016/j.molonc.2016.01.007.
55. Harouaka RA, Nisic M, Zheng S. Circulating Tumor Cell Enrichment Based on Physical Properties. 2013;(X). doi:10.1177/2211068213494391.
56. Ligthart ST, Coumans FA, Bidard FC, et al. Circulating Tumor Cells Count and Morphological Features in Breast, Colorectal and Prostate Cancer. *PLoS One*. 2013;8(6):e67148. doi:10.1371/journal.pone.0067148.
57. Shim S, Stemke-Hale K, Tsimberidou AM, Noshari J, Anderson TE, Gascoyne PRC. Antibody-independent isolation of circulating tumor cells by continuous-flow dielectrophoresis. *Biomicrofluidics*. 2013;7(1):11807. doi:10.1063/1.4774304.
58. Abonnenc M, Manaresi N, Borgatti M, et al. Programmable Interactions of Functionalized Single Bioparticles in a Dielectrophoresis-Based Microarray Chip. 2013. doi:10.1021/ac401296m.
59. Duffy DC, Mcdonald JC, Schueller OJA, Whitesides GM. Rapid Prototyping of Microfluidic Systems in Poly (dimethylsiloxane). 1998;70(23):4974-4984.

60. Whitesides GM. The origins and the future of microfluidics. *Nature*. 2006;442(7101):368-373. doi:10.1038/nature05058.
61. Cho H, Kim J, Song H, Sohn KY, Jeon M, Han KH. Microfluidic technologies for circulating tumor cell isolation. *Analyst*. 2018;143(13):2936-2970. doi:10.1039/c7an01979c.
62. Stott SL, Hsu C-HC-H, Tsukrov DI, et al. Isolation of circulating tumor cells using a. *October*. 2010;107(35):18392-18397. doi:10.1073/pnas.1012539107/-/DCSupplemental.www.pnas.org/cgi/doi/10.1073/pnas.1012539107.
63. Alix-Panabières C, Pantel K. Challenges in circulating tumour cell research. *Nat Rev Cancer*. 2014;14(9):623-631. doi:10.1038/nrc3820.
64. Swennenhuis JF, Dalum G Van, Zeune LL, et al. Expert Review of Molecular Diagnostics Improving the CellSearch ® system Improving the CellSearch ® system. *Expert Rev Mol Diagn*. 2016;16(12):1291-1305. doi:10.1080/14737159.2016.1255144.
65. Zeune L, Van Dalum G, Decraene C, et al. Quantifying HER-2 expression on circulating tumor cells by ACCEPT. *PLoS One*. 2017;12(10):1-12. doi:10.1371/journal.pone.0186562.
66. Werner SL, Graf RP, Landers M, et al. Analytical Validation and Capabilities of the Epic CTC Platform: Enrichment-Free Circulating Tumour Cell Detection and Characterization. *J Circ Biomarkers*. 2015:1. doi:10.5772/60725.
67. Alix-Panabières C, Vendrell J-P, Slijper M, et al. Full-length cytokeratin-19 is released by human tumor cells: a potential role in metastatic progression of breast cancer. *Breast Cancer Res*. 2009;11(3):R39. doi:10.1186/bcr2326.
68. Alix-panabières C, Pantel K. Liquid biopsy in cancer patients : advances in capturing viable CTCs for functional studies using the EPISPOT assay Liquid biopsy in cancer patients : advances in capturing viable CTCs for functional studies using the EPISPOT assay. 2015;7159(September). doi:10.1586/14737159.2015.1091729.
69. Tulley S, Zhao Q, Dong H, Pearl ML, Chen W-T. Vita-Assay{\texttrademark} Method of Enrichment and Identification of Circulating Cancer Cells/Circulating Tumor Cells (CTCs). In: Cao J, ed. *Breast Cancer: Methods and Protocols*. New York, NY: Springer New York; 2016:107-119. doi:10.1007/978-1-4939-3444-7_9.
70. Rossi E, Rugge M, Facchinetti A, et al. Retaining the long-survive capacity of Circulating Tumor Cells (CTCs) followed by xeno-transplantation: not only from metastatic cancer of the breast but also of prostate cancer patients. *Oncoscience*.

2014;1(1):49-56. doi:10.18632/oncoscience.8.

71. Hodgkinson CL, Morrow CJ, Li Y, et al. Tumorigenicity and genetic profiling of circulating tumor cells in small-cell lung cancer. *Nat Med*. 2014;20(8):897-903. doi:10.1038/nm.3600.

72. Morrow CJ, Trapani F, Metcalf RL, et al. Tumourigenic non-small-cell lung cancer mesenchymal circulating tumour cells: A clinical case study. *Ann Oncol*. 2016;27(6):1155-1160. doi:10.1093/annonc/mdw122.

73. Baccelli I, Schneeweiss A, Riethdorf S, et al. Identification of a population of blood circulating tumor cells from breast cancer patients that initiates metastasis in a xenograft assay. *Nat Biotechnol*. 2013;31(6):539-544. doi:10.1038/nbt.2576.

74. Barnard ME, Boeke CE, Tamimi RM. Established breast cancer risk factors and risk of intrinsic tumor subtypes. *Biochim Biophys Acta - Rev Cancer*. 2015;1856(1):73-85. doi:10.1016/j.bbcan.2015.06.002.

75. Polzer B, Medoro G, Pasch S, et al. Molecular profiling of single circulating tumor cells with diagnostic intention. *EMBO Mol Med*. 2014;6(11):1371-1386. doi:10.15252/emmm.201404033.

76. Kondo Y, Hayashi K, Kawakami K, Miwa Y, Hayashi H, Yamamoto M. KRAS mutation analysis of single circulating tumor cells from patients with metastatic colorectal cancer. *BMC Cancer*. 2017;17(1):311. doi:10.1186/s12885-017-3305-6.

77. Yu M, Bardia A, Wittner BS, et al. Circulating breast tumor cells exhibit dynamic changes in epithelial and mesenchymal composition. *Science (80-)*. 2013;339(6119):580-584. doi:10.1126/science.1228522.

78. Miyamoto DT, Zheng Y, Wittner BS, et al. RNA-Seq of single prostate CTCs implicates noncanonical Wnt signaling in antiandrogen resistance. *Science (80-)*. 2015;349(6254):1351-1356. doi:10.1126/science.aab0917.

79. Kalinich M, Bhan I, Kwan TT, et al. An RNA-based signature enables high specificity detection of circulating tumor cells in hepatocellular carcinoma. *Proc Natl Acad Sci*. 2017;114(5):1123-1128. doi:10.1073/pnas.1617032114.

80. Bulfoni M, Turetta M, Del Ben F, Di Loreto C, Beltrami AP, Cesselli D. Dissecting the heterogeneity of circulating tumor cells in metastatic breast cancer: Going far beyond the needle in the Haystack. *Int J Mol Sci*. 2016. doi:10.3390/ijms17101775.

81. Bidard FC, Proudhon C, Pierga JY. Circulating tumor cells in breast cancer. *Mol Oncol*. 2016;10(3):418-430. doi:10.1016/j.molonc.2016.01.001.

82. Neumann MHD, Bender S, Krahn T, Schlange T. ctDNA and CTCs in Liquid Biopsy

– Current Status and Where We Need to Progress. *Comput Struct Biotechnol J*. 2018;16:190-195. doi:10.1016/J.CSBJ.2018.05.002.

83. Bidard F-C, Fehm T, Ignatiadis M, et al. Clinical application of circulating tumor cells in breast cancer: overview of the current interventional trials. *Cancer Metastasis Rev*. 2013;32(1-2):179-188. doi:10.1007/s10555-012-9398-0.
84. Romiti A, Raffa S, Di Rocco R, et al. Circulating tumor cells count predicts survival in colorectal cancer patients. *J Gastrointestin Liver Dis*. 2014;23(3):279-284. doi:10.15403/jgld.2014.1121.233.arom1.
85. Cohen SJ, Punt CJA, Iannotti N, et al. Relationship of circulating tumor cells to tumor response, progression-free survival, and overall survival in patients with metastatic colorectal cancer. *J Clin Oncol*. 2008;26(19):3213-3221. doi:10.1200/JCO.2007.15.8923.
86. Lorente D, Olmos D, Mateo J, et al. Decline in Circulating Tumor Cell Count and Treatment Outcome in Advanced Prostate Cancer. *Eur Urol*. 2016;70(6):985-992. doi:10.1016/j.eururo.2016.05.023.
87. Krebs MG, Sloane R, Priest L, et al. Evaluation and prognostic significance of circulating tumor cells in patients with non-small-cell lung cancer. *J Clin Oncol*. 2011;29(12):1556-1563. doi:10.1200/JCO.2010.28.7045.
88. Lucci A, Hall CS, Lodhi AK, et al. Circulating tumour cells in non-metastatic breast cancer: A prospective study. *Lancet Oncol*. 2012;13(7):688-695. doi:10.1016/S1470-2045(12)70209-7.
89. Lu Y, Wang P, Peng J, Wang X, Zhu Y, Shen N. Meta-analysis Reveals the Prognostic Value of Circulating Tumour Cells Detected in the Peripheral Blood in Patients with Non-Metastatic Colorectal Cancer. *Sci Rep*. 2017;7(1):905. doi:10.1038/s41598-017-01066-y.
90. Van Dalum G, Stam G-J, Scholten LFA, et al. Importance of circulating tumor cells in newly diagnosed colorectal cancer. *Int J Oncol*. 2015;46(3):1361-1368. doi:10.3892/ijo.2015.2824.
91. Riethdorf S, Müller V, Loibl S, et al. Prognostic impact of circulating tumor cells for breast cancer patients treated in the neoadjuvant "Geparquattro" trial. *Clin Cancer Res*. 2017;(14):clincanres.0255.2017. doi:10.1158/1078-0432.CCR-17-0255.
92. Smerage JB, Barlow WE, Hortobagyi GN, et al. Circulating tumor cells and response to chemotherapy in metastatic breast cancer: SWOG S0500. *J Clin Oncol*.

2014;32(31):3483-3489. doi:10.1200/JCO.2014.56.2561.

93. Scher HI, Lu D, Schreiber NA, et al. Association of AR-V7 on circulating tumor cells as a treatment-specific biomarker with outcomes and survival in castration-resistant prostate cancer. *JAMA Oncol*. 2016;2(11):1441-1449. doi:10.1001/jamaoncol.2016.1828.

94. Sullivan LB, Gui DY, Van Der Heiden MG. Altered metabolite levels in cancer: Implications for tumour biology and cancer therapy. *Nat Rev Cancer*. 2016;16(11):680-693. doi:10.1038/nrc.2016.85.

95. Ward PS, Thompson CB. Metabolic Reprogramming : A Cancer Hallmark Even Warburg Did Not Anticipate. *Cancer Cell*. 2012;21(3):297-308. doi:10.1016/j.ccr.2012.02.014.

96. Osthus RC, Shim H, Kim S, et al. Deregulation of glucose transporter 1 and glycolytic gene expression by c-Myc. *J Biol Chem*. 2000;275(29):21797-21800. doi:10.1074/jbc.C000023200.

97. King A, Selak MA, Gottlieb E. Succinate dehydrogenase and fumarate hydratase: Linking mitochondrial dysfunction and cancer. *Oncogene*. 2006;25(34):4675-4682. doi:10.1038/sj.onc.1209594.

98. Warburg O. The Metabolism of Carcinoma Cells. *J Cancer Res*. 1925;9:148-163. doi:10.1158/jcr.1925.148.

99. Gatenby RA, Gillies RJ. Why do cancers have high aerobic glycolysis? *Nat Rev Cancer*. 2004;4(11):891-899. doi:10.1038/nrc1478.

100. Ben-Haim S, Ell P. 18F-FDG PET and PET/CT in the Evaluation of Cancer Treatment Response. *J Nucl Med*. 2008;50(1):88-99. doi:10.2967/jnumed.108.054205.

101. Kelloff GJ, Hoffman JM, Johnson B, et al. Progress and Promise of FDG-PET Imaging for Cancer Patient Management and Oncologic Drug Development Management and Oncologic Drug Development. 2005;11(8):2785-2808. doi:10.1158/1078-0432.CCR-04-2626.

102. Shestov AA, Liu X, Ser Z, et al. Quantitative determinants of aerobic glycolysis identify flux through the enzyme GAPDH as a limiting step. *Elife*. 2014;3(July2014):1-18. doi:10.7554/eLife.03342.

103. DeBerardinis RJ. Is cancer a disease of abnormal cellular metabolism? New angles on an old idea. *Genet Med*. 2008;10(11):767-777. doi:10.1097/GIM.0b013e31818b0d9b.

104. Adekola K, Rosen ST, Shanmugam M. Glucose transporters in cancer metabolism. *Curr Opin Oncol*. 2012;24(6):650-654. doi:10.1097/CCO.0b013e328356da72.
105. Macheda ML, Rogers S, Best JD. Molecular and cellular regulation of glucose transporter (GLUT) proteins in cancer. *J Cell Physiol*. 2005;202(3):654-662. doi:10.1002/jcp.20166.
106. Patra KC, Wang Q, Bhaskar PT, et al. Hexokinase 2 is required for tumor initiation and maintenance and its systemic deletion is therapeutic in mouse models of cancer. *Cancer Cell*. 2013;24(2):213-228. doi:10.1016/j.ccr.2013.06.014.
107. Hay N. Reprogramming glucose metabolism in cancer: can it be exploited for cancer therapy? *Nat Rev Cancer*. 2016;16(10):635-649. doi:10.1038/nrc.2016.77.
108. Schwartzenberg-bar-yoseph F, Armoni M, Karnieli E. The Tumor Suppressor p53 Down-Regulates Glucose Transporters GLUT1 and GLUT4 Gene Expression The Tumor Suppressor p53 Down-Regulates Glucose Transporters GLUT1 and GLUT4 Gene Expression. *Cancer Res*. 2004:2627-2633. doi:10.1158/0008-5472.CAN-03-0846.
109. Mathupala SP, Rempel A, Pedersen PL. Glucose catabolism in cancer cells: Identification and characterization of a marked activation response of the type II hexokinase gene to hypoxic conditions. *J Biol Chem*. 2001;276(46):43407-43412. doi:10.1074/jbc.M108181200.
110. Bensaad K, Tsuruta A, Selak MA, et al. TIGAR, a p53-Inducible Regulator of Glycolysis and Apoptosis. *Cell*. 2006;126(1):107-120. doi:10.1016/j.cell.2006.05.036.
111. Itahana Y, Itahana K. Emerging roles of p53 family members in glucose metabolism. *Int J Mol Sci*. 2018;19(3):1-22. doi:10.3390/ijms19030776.
112. Chalhoub N, Baker SJ. PTEN and the PI3-kinase pathway in cancer. *Annu Rev Pathol*. 2009;4(1):127-150. doi:10.1146/annurev.pathol.4.110807.092311.
113. Elstrom RL, Bauer DE, Buzzai M, et al. Akt stimulates aerobic glycolysis in cancer cells. *Cancer Res*. 2004;64(11):3892-3899. doi:10.1158/0008-5472.CAN-03-2904.
114. Buzzai M, Bauer DE, Jones RG, et al. The glucose dependence of Akt-transformed cells can be reversed by pharmacologic activation of fatty acid b -oxidation. 2005;(October 2004):4165-4173. doi:10.1038/sj.onc.1208622.
115. Kimmelman AC. Metabolic dependencies in RAS-driven cancers. *Clin Cancer Res*. 2015;21(8):1828-1834. doi:10.1158/1078-0432.CCR-14-2425.
116. Pylayeva-Gupta Y, Grabocka E, Bar-Sagi D. RAS oncogenes: Weaving a

tumorigenic web. *Nat Rev Cancer*. 2011;11(11):761-774. doi:10.1038/nrc3106.

117. Blum R, Jacob-Hirsch J, Amariglio N, Rechavi G, Kloog Y. Ras inhibition in glioblastoma down-regulates hypoxia-inducible factor-1α, causing glycolysis shutdown and cell death. *Cancer Res*. 2005;65(3):999-1006. doi:65/3/999.
118. Chen C, Pore N, Behrooz A, Ismail-Beigi F, Maity A. Regulation of glut1 mRNA by hypoxia-inducible factor-1: Interaction between H-ras and hypoxia. *J Biol Chem*. 2001;276(12):9519-9525. doi:10.1074/jbc.M010144200.
119. Chun SY, Johnson C, Washburn JG, Cruz-Correa MR, Dang DT, Dang LH. Oncogenic KRAS modulates mitochondrial metabolism in human colon cancer cells by inducing HIF-1α and HIF-2α target genes. *Mol Cancer*. 2010;9(1):293. doi:10.1186/1476-4598-9-293.
120. Kikuchi H, Pino MS, Min Z, Shirasawa S, Chung DC. Oncogenic KRAS and BRAF differentially regulate hypoxia-inducible factor-1α and -2α in colon cancer. *Cancer Res*. 2009;69(21):8499-8506. doi:10.1158/0008-5472.CAN-09-2213.
121. Sears R, Leone G, DeGregori J, Nevins JR. Ras enhances Myc protein stability. *Mol Cell*. 1999;3(2):169-179. doi:10.1016/S1097-2765(00)80308-1.
122. Chiche J, Brahimi-Horn MC, Pouysségur J. Tumour hypoxia induces a metabolic shift causing acidosis: A common feature in cancer. *J Cell Mol Med*. 2010;14(4):771-794. doi:10.1111/j.1582-4934.2009.00994.x.
123. Gillies RJ, Robey I, Gatenby RA. Causes and consequences of increased glucose metabolism of cancers. *J Nucl Med*. 2008;49 Suppl 2(6):24S-42S. doi:10.2967/jnumed.107.047258.
124. Cardone R a, Casavola V, Reshkin SJ. The role of disturbed pH dynamics and the Na+/H+ exchanger in metastasis. *Nat Rev Cancer*. 2005;5(10):786-795. doi:10.1038/nrc1713.
125. Sáenz-de-Santa-María I, Bernardo-Castiñeira C, Secades P, et al. Clinically relevant HIF-1α-dependent metabolic reprogramming in oropharyngeal squamous cell carcinomas includes coordinated activation of CAIX and the miR-210/ISCU signaling axis, but not MCT1 and MCT4 upregulation. *Oncotarget*. 2017;(January). doi:10.18632/oncotarget.14629.
126. Anderson M, Moshnikova A, Engelman DM, Reshetnyak YK, Andreev OA. Probe for the measurement of cell surface pH in vivo and ex vivo. *Proc Natl Acad Sci*. 2016;113(29):8177-8181. doi:10.1073/pnas.1608247113.
127. Longo DL, Bartoli A, Consolino L, et al. In vivo imaging of tumor metabolism and

acidosis by combining PET and MRI-CEST pH imaging. *Cancer Res*. 2016;76(22):6463-6470. doi:10.1158/0008-5472.CAN-16-0825.

128. Newell K, Franchi A, Pouysségur J, Tannock I. Studies with glycolysis-deficient cells suggest that production of lactic acid is not the only cause of tumor acidity. *Proc Natl Acad Sci U S A*. 1993;90(3):1127-1131. doi:10.1073/pnas.90.3.1127.
129. Yamagata M, Hasuda K, Stamato T, Tannock IF. The contribution of lactic acid to acidification of tumours: Studies of variant cells lacking lactate dehydrogenase. *Br J Cancer*. 1998;77(11):1726-1731. doi:10.1038/bjc.1998.289.
130. Webb BA, Chimenti M, Jacobson MP, Barber DL. Dysregulated pH: a perfect storm for cancer progression. *Nat Rev Cancer*. 2011;11(9):671-677. doi:10.1038/nrc3110.
131. Parks SK, Chiche J, Pouysségur J. Disrupting proton dynamics and energy metabolism for cancer therapy. *Nat Rev Cancer*. 2013;13(9):611-623. doi:10.1038/nrc3579.
132. Reshkin SJ, Bellizzi A, Caldeira S, et al. Na+/H+ exchanger-dependent intracellular alkalinization is an early event in malignant transformation and plays an essential role in the development of subsequent transformation-associated phenotypes. *FASEB J*. 2000;14(14):2185-2197. doi:10.1096/fj.00-0029com.
133. Halestrap AP. The monocarboxylate transporter family-Structure and functional characterization. *IUBMB Life*. 2012;64(1):1-9. doi:10.1002/iub.573.
134. Pinheiro C, Longatto-Filho A, Azevedo-Silva J, Casal M, Schmitt FC, Baltazar F. Role of monocarboxylate transporters in human cancers: State of the art. *J Bioenerg Biomembr*. 2012;44(1):127-139. doi:10.1007/s10863-012-9428-1.
135. Boidot R, Veģran F, Meulle A, et al. Regulation of monocarboxylate transporter MCT1 expression by p53 mediates inward and outward lactate fluxes in tumors. *Cancer Res*. 2012;72(4):939-948. doi:10.1158/0008-5472.CAN-11-2474.
136. Granja S, Tavares-Valente D, Queirós O, Baltazar F. Value of pH regulators in the diagnosis, prognosis and treatment of cancer. *Semin Cancer Biol*. 2017;43:17-34. doi:10.1016/j.semcancer.2016.12.003.
137. Chiche J, Ilc K, Laferrière J, et al. Hypoxia-inducible carbonic anhydrase IX and XII promote tumor cell growth by counteracting acidosis through the regulation of the intracellular pH. *Cancer Res*. 2009;69(1):358-368. doi:10.1158/0008-5472.CAN-08-2470.
138. Lock FE, McDonald PC, Lou Y, et al. Targeting carbonic anhydrase IX depletes breast cancer stem cells within the hypoxic niche. *Oncogene*. 2013;32(44):5210-

5219. doi:10.1038/onc.2012.550.

139. Estrella V, Chen T, Lloyd M, et al. Acidity generated by the tumor microenvironment drives local invasion. *Cancer Res*. 2013;73(5):1524-1535. doi:10.1158/0008-5472.CAN-12-2796.

140. Fukumura D, Xu L, Chen Y, Gohongi T, Seed B, Jain RK. Hypoxia and Acidosis Independently Up-Regulate Vascular Endothelial Growth Factor Transcription in Brain Tumors in Vivo Advances in Brief Hypoxia and Acidosis Independently Up-Regulate Vascular Endothelial Growth Factor Transcription in Brain Tumors in Vi. 2001:6020-6024.

141. Xu L, Fukumura D, Jain RK. Acidic extracellular pH induces vascular endothelial growth factor (VEGF) in human glioblastoma cells via ERK1/2 MAPK signaling pathway. Mechanism of low pH-induced VEGF. *J Biol Chem*. 2002;277(13):11368-11374. doi:10.1074/jbc.M108347200.

142. Martinez-Outschoorn UE, Peiris-Pagés M, Pestell RG, Sotgia F, Lisanti MP. Cancer metabolism: A therapeutic perspective. *Nat Rev Clin Oncol*. 2017;14(1):11-31. doi:10.1038/nrclinonc.2016.60.

143. Kolosenko I, Avnet S, Baldini N, Viklund J, De Milito A. Therapeutic implications of tumor interstitial acidification. *Semin Cancer Biol*. 2017;43:119-133. doi:10.1016/j.semcancer.2017.01.008.

144. Chokkalingam V, Tel J, Wimmers F, et al. Probing cellular heterogeneity in cytokine-secreting immune cells using droplet-based microfluidics. *Lab Chip*. 2013;13(24):4740-4744. doi:10.1039/c3lc50945a.

145. Mazutis L, Gilbert J, Ung WL, Weitz DA, Griffiths AD, Heyman JA. Single-cell analysis and sorting using droplet-based microfluidics. *Nat Protoc*. 2013;8(5):870-891. doi:doi:10.1038/nprot.2013.046.

146. Baret J-C, Miller OJ, Taly V, et al. Fluorescence-activated droplet sorting (FADS): efficient microfluidic cell sorting based on enzymatic activity. *Lab Chip*. 2009;9(13):1850-1858. doi:10.1039/b902504a.

147. Del Ben F, Turetta M, Celetti G, et al. A Method for Detecting Circulating Tumor Cells Based on the Measurement of Single-Cell Metabolism in Droplet-Based Microfluidics. *Angew Chemie - Int Ed*. 2016;55(30):8581-8584. doi:10.1002/anie.201602328.

148. Theberge AB, Courtois F, Schaerli Y, et al. Microdroplets in microfluidics: An evolving platform for discoveries in chemistry and biology. *Angew Chemie - Int Ed*.

2010;49(34):5846-5868. doi:10.1002/anie.200906653.

149. Gatenby RA, Gawlinski ET, Gmitro AF, Kaylor B, Gillies RJ. Acid-mediated tumor invasion: A multidisciplinary study. *Cancer Res*. 2006;66(10):5216-5223. doi:10.1158/0008-5472.CAN-05-4193.

150. Fabian C, Koetz L, Favaro E, Indraccolo S, Mueller-Klieser W, Sattler UGA. Protein profiles in human ovarian cancer cell lines correspond to their metabolic activity and to metabolic profiles of respective tumor xenografts. *FEBS J*. 2012;279(5):882-891. doi:10.1111/j.1742-4658.2012.08479.x.

151. Bidard F-C, Peeters DJ, Fehm T, et al. Clinical validity of circulating tumour cells in patients with metastatic breast cancer: a pooled analysis of individual patient data. *Lancet Oncol*. 2014;15(4):406-414. doi:10.1016/S1470-2045(14)70069-5.

152. Rossi E, Basso U, Celadin R, et al. M30 neoepitope expression in epithelial cancer: Quantification of apoptosis in circulating tumor cells by CellSearch analysis. *Clin Cancer Res*. 2010;16(21):5233-5243. doi:10.1158/1078-0432.CCR-10-1449.

153. Antonarakis ES, Lu C, Wang H, et al. AR-V7 and Resistance to Enzalutamide and Abiraterone in Prostate Cancer. *N Engl J Med*. 2014;371(11):1028-1038. doi:10.1056/NEJMoa1315815.

154. Fehm T, Müller V, Aktas B, et al. HER2 status of circulating tumor cells in patients with metastatic breast cancer: A prospective, multicenter trial. *Breast Cancer Res Treat*. 2010;124(2):403-412. doi:10.1007/s10549-010-1163-x.

155. Beije N, Onstenk W, Kraan J, et al. Prognostic Impact of HER2 and ER Status of Circulating Tumor Cells in Metastatic Breast Cancer Patients with a HER2-Negative Primary Tumor. *Neoplasia*. 2016;18(11):647-653. doi:http://dx.doi.org/10.1016/j.neo.2016.08.007.

156. Zhang L, Riethdorf S, Wu G, et al. Meta-analysis of the prognostic value of circulating tumor cells in breast cancer. *Clin Cancer Res*. 2012;18(20):5701-5710. doi:10.1158/1078-0432.CCR-12-1587.

157. Budd GT, Cristofanilli M, Ellis MJ, et al. Circulating tumor cells versus imaging - Predicting overall survival in metastatic breast cancer. *Clin Cancer Res*. 2006;12(21):6403-6409. doi:10.1158/1078-0432.CCR-05-1769.

158. Gatenby RA, Gillies RJ. A microenvironmental model of carcinogenesis. *Nat Rev Cancer*. 2008;8(1):56-61. doi:10.1038/nrc2255.

159. Debs BE, Utharala R, Balyasnikova I V., Griffiths a. D, Merten C a. Functional single-cell hybridoma screening using droplet-based microfluidics. *Proc Natl Acad*

Sci. 2012;109:11570-11575. doi:10.1073/pnas.1204514109.

160. Mongersun A, Smeenk I, Pratx G, Asuri P, Abbyad P. Droplet Microfluidic Platform for the Determination of Single-Cell Lactate Release. *Anal Chem*. 2016;IN PRESS. doi:10.1021/acs.analchem.5b04681.

161. Tang Y, Wang Z, Li Z, et al. High-throughput screening of rare metabolically active tumor cells in pleural effusion and peripheral blood of lung cancer patients. *Proc Natl Acad Sci*. 2017;114(14):2544-2549. doi:10.1073/pnas.1703650114.

162. Turetta M, Bulfoni M, Brisotto G, et al. Assessment of the Mutational Status of NSCLC Using Hypermetabolic Circulating Tumor Cells. *Cancers (Basel)*. 2018;10(8):270. doi:10.3390/cancers10080270.

163. Chen J, Cao S, Situ B, et al. Metabolic reprogramming-based characterization of circulating tumor cells in prostate cancer. *J Exp Clin Cancer Res*. 2018;37(1):127. doi:10.1186/s13046-018-0789-0.

164. Cai H, Peng F. 2-NBDG fluorescence imaging of hypermetabolic circulating tumor cells in mouse xenograft model of breast cancer. *J Fluoresc*. 2013;23(1):213-220. doi:10.1007/s10895-012-1136-z.

165. Zhang Y, Tang Y, Sun S, et al. Single-Cell Codetection of Metabolic Activity, Intracellular Functional Proteins, and Genetic Mutations from Rare Circulating Tumor Cells. *Anal Chem*. 2015;87(19):9761-9768. doi:10.1021/acs.analchem.5b01901.

166. Gallina ME, Kim TJ, Shelor M, et al. Toward a Droplet-Based Single-Cell Radiometric Assay. *Anal Chem*. 2017;89(12):6472-6481. doi:10.1021/acs.analchem.7b00414.

ACKNOWLEDGMENTS

This thesis would not have been possible without the guidance and support from many different people. First of all, I would like to thank Prof. Alfonso Colombatti, who gave me the opportunity to work on this research field. Thank you for giving me all the freedom and independence to develop this project, the right advices when I was discouraged and for teaching me that you have to fight for what you believe in.

A great thanks to all the members of the lab at CRO Aviano National Cancer Institute. Fabio and Matteo for their technical support and for making me realize how stubborn I can be and Eva and Michela for their essential work and opinion that have helped improving this work. A special thanks to Dr. Agostino Steffan, who has been always ready to help me out from any kind of problems.

I would like to extend my gratitude to the members of the CTC-lab at the Veneto Institute of Oncology IOV-IRCCS of Padova. Thanks to Dr. Rita Zamarchi for her continuous encouragement and timely guidance to explore this field of research. Thanks to Betta for her endless patient, for giving me time for unscheduled meetings and all her countless message of support. Cristina, Riccardo and Maria Chiara for their valuable help with the experiments, all the coffees and the laughs.

Another thanks go to my friends, those present daily and those that have been always close to me, no matter the distance and time. A special thanks goes to Giulia for all the constructive discussions, her constant motivation, the time she spent listening to my complaints, her honesty and for letting me focus on my objectives when I was getting lost. Thanks to Ale and Enzo, Michela and Adriano for their sincere love, support, advices and for being always there when I needed.

Last but not least, I wish to express my gratitude to my parents and my brother Nicola for their never-ending support, love and motivation. Thanks for teaching me that from working hard, honestly and with passion great satisfaction will come. Thanks for believing in me and all the sacrifice you made towards achieving this goal.

RINGRAZIAMENTI

Questa tesi non sarebbe stata possibile senza la guida e il supporto di molte persone. Prima di tutto, vorrei ringraziare il Prof. Alfonso Colombatti, che mi ha dato l'opportunità di lavorare su questo ambito di ricerca. Grazie per avermi dato tutta la libertà e l'indipendenza per sviluppare questo progetto, i giusti consigli quando ero scoraggiata e per avermi insegnato che si deve combattere per ciò in cui si crede.

Un grande ringraziamento a tutti i membri del laboratorio del CRO di Aviano. Fabio e Matteo per il loro supporto tecnico e per avermi fatto capire quanto posso essere testarda e Eva e Michela per il loro fondamentale aiuto e le loro opinioni che hanno contribuito a migliorare questo lavoro. Un ringraziamento speciale al Dott. Agostino Steffan, che è sempre stato pronto ad aiutarmi per ogni tipo di problema.

Vorrei esprimere la mia gratitudine ai membri del laboratorio CTC dell'Istituto Oncologico Veneto di Padova. Grazie alla Dott.ssa Rita Zamarchi per il suo continuo incoraggiamento e per avermi guidato nella conoscenza di questo campo di ricerca. Grazie a Betta per la sua infinita pazienza e per gli innumerevoli messaggi di supporto. Cristina, Riccardo e Maria Chiara per il loro prezioso aiuto con gli esperimenti, i caffè e le risate.

Un altro grazie va ai miei amici, quelli presenti ogni giorno e quelli che mi sono sempre stati vicini, indipendentemente dalla distanza e dal tempo. Un ringraziamento speciale va a Giulia per tutte le discussioni costruttive, la sua costante motivazione, il tempo che ha trascorso ascoltando le mie lamentele, la sua onestà e per avermi fatto focalizzare sui miei obiettivi quando mi stavo perdendo. Grazie ad Ale ed Enzo, Michela e Adriano per la loro sincera amicizia, il supporto, i consigli e per esserci sempre stati quando necessario.

Ultimo ma non meno importante, desidero esprimere la mia gratitudine ai miei genitori e a mio fratello Nicola per il loro sostegno, amore e continua motivazione. Grazie per avermi insegnato che lavorando sodo, onestamente e con passione si ottengono grandi soddisfazioni. Grazie per aver creduto in me e per tutto l’aiuto che mi avete dato per permettermi di raggiungere questo obiettivo.